Molecular phylogeny and species delimitation of the genus *Dicerapanorpa* (Mecoptera: Panorpidae)

GUI-LIN HU[1], KAI GAO[1], JI-SHEN WANG[1], PAUL D. N. HEBERT[2] and BAO-ZHEN HUA[1,*,]

[1]*Key Laboratory of Plant Protection Resources and Pest Management, Ministry of Education, College of Plant Protection, Northwest A&F University, Yangling, Shaanxi, China*
[2]*Centre for Biodiversity Genomics, University of Guelph, Guelph, ON, Canada*

Given that species is the fundamental unit in systematic biology, rigorous species delimitation is crucial for taxonomic studies, yet routine species delimitation remains an ongoing challenge in the taxonomic practice of insects. The two-horned scorpionfly *Dicerapanorpa* is a small genus in Panorpidae (Mecoptera) endemic to the Qinling-Bashan and Hengduan mountains, a biodiversity hotspot. However, species of *Dicerapanorpa* are difficult to delineate owing to marked intraspecific variation and interspecific similarity. Here, we investigate the diversity and species boundaries of *Dicerapanorpa* using an integrative approach based on DNA barcoding, morphological, geometric morphometric and molecular phylogenetic analyses. This integrative analyses confirmed the 13 described species of *Dicerapanorpa* and revealed three new species: **_Dicerapanorpa lativalva_ sp. nov.**, **_Dicerapanorpa hualongshana_ sp. nov.** and **_Dicerapanorpa minshana_ sp. nov.** Most molecular operational taxonomic units are in congruence with morphological clusters. Possible reasons for several discordances in *Dicerapanorpa* are tentatively discussed.

ADDITIONAL KEYWORDS: DNA barcoding – integrative taxonomy – morphology – morphometry.

INTRODUCTION

Given that species is the fundamental unit of biology, rigorous species delimitation is crucial for biodiversity studies, conservation programmes and ecological and evolutionary research (Isaac *et al.*, 2004; de Queiroz, 2005, 2007; Bickford *et al.*, 2007; Wiens, 2007; Bortolus, 2008). More than 25 species concepts have been proposed during the past few decades, but many of these are difficult to apply in reality and some are incompatible, leading to different conclusions concerning the boundaries and number of species (de Queiroz, 2007). Although the unified species concept is receiving more and more support (de Queiroz, 2007), routine species delimitation remains an ongoing challenge in the taxonomic practice of many insect groups to date. Recently, integrative taxonomy has been adopted by numerous insect taxonomists to delimit species boundaries in many insect groups

with good results, including the fruit fly *Bactrocera dorsalis* complex (Schutze *et al.*, 2015, 2017) and jumping bristletails (Dejaco *et al.*, 2016).

The two-horned scorpionfly, *Dicerapanorpa* Zhong & Hua, 2013, is a small genus of the diverse family Panorpidae in Mecoptera (Zhong & Hua, 2013a; Wang & Hua, 2017). Species of *Dicerapanorpa*, mainly diagnosed by two anal horns on tergum VI in males, are endemic to the Qinling-Bashan and Hengduan Mountain ranges, a biodiversity hotspot. The monophyly of the genus has been confirmed by both molecular data (Hu *et al.*, 2015; Miao *et al.*, 2019) and morphological studies (Ma *et al.*, 2009, 2011, 2012). The larvae of *Dicerapanorpa* are eruciform with annulated processes on the dorsum, which might have adaptive significance for fossorial and soil-living habits (Ma *et al.*, 2014). The male adults control the females during mating with a notal organ on the third abdominal tergum and two finger-like anal horns on the sixth tergum, and offer salivary masses as nuptial gifts to prolong copulation (Zhong *et al.*, 2015).

The members of *Dicerapanorpa* can be categorized into two groups (Zhong & Hua, 2013a; Hu &

Hua, 2019; Hu *et al.*, 2019b). The first group (the *Dicerapanorpa magna* Chou in Chou *et al.*, 1981 group), characterized by yellowish wings with distinct markings and a rostrum lacking distinct longitudinal stripes, is nearly restricted to the Qinling-Bashan Mountains, where it inhabits dense forests with herbaceous groundcover. In contrast, the second group [the *Dicerapanorpa diceras* (MacLachlan, 1894) group], distinguished by hyaline wings without distinct markings and a rostrum with two distinct lateral stripes, is most abundant in the Hengduan Mountains, where it occurs in open areas with direct sunlight, especially near river margins.

Species of *Dicerapanorpa* are largely diagnosed by the male adult morphological features, whereas the female morphology has received little investigation. In fact, some sympatric species exhibit morphological stasis or homoplasy owing to similar selective pressure, making the species delimitation particularly difficult. For example, the sympatric *Dicerapanorpa macula* Hu, Wang & Hua, 2019 and *Dicerapanorpa zhongdianensis* Hu, Wang & Hua, 2019 occur in Shangri-La County, Yunnan Province and exhibit similar body shape and wing coloration and pattern (Hu *et al.*, 2019b), leading to difficulty in discriminating between the conspecific and heterospecific females. Moreover, detailed studies of *D. magna* revealed considerable variation in its external morphology (e.g. wing shape) and internal anatomy (e.g. number of female ovarioles and male salivary gland tubes) (Hou & Hua, 2008; Ma *et al.*, 2011; Liu *et al.*, 2016). A phylogeographical study further suggested that incipient speciation has probably occurred in *D. magna* (Hu *et al.*, 2019a). The interspecific morphological similarities and intraspecific variations blurred the distinction between geographical population-level variation and species-level divergence in *Dicerapanorpa*. Therefore, the genus *Dicerapanorpa* needs to be investigated comprehensively through an integrative approach.

DNA barcoding (Hebert *et al.*, 2003a, b) has disentangled taxonomic disputes and accelerated the discovery of new species in numerous taxa (e.g. Smith *et al.*, 2006; Witt *et al.*, 2006; Hsu *et al.*, 2013; Mendoza *et al.*, 2016). For the bulk of undescribed biodiversity, the DNA barcoding approach was proposed to produce potential species [i.e. operational taxonomic units (OTUs)] for approximating species description (Goldstein & DeSalle, 2011; Puillandre *et al.*, 2012b). Molecular OTUs were subsequently evaluated with various criteria, such as morphological, geometric morphometric, geographical and phylogenetic data. Conclusive concordance among different disciplines reinforces the robustness of species hypotheses, and discordance over the number and demarcation of species

is resolved by invoking evolutionary explanations (Schlick-Steiner *et al.*, 2010; Carstens *et al.*, 2013). The integrative approach with multiple independent lines of evidence has effectively delivered significant advances in the resolution of taxonomically intricate instances and uncovering complex evolutionary histories (Dayrat, 2005; Padial *et al.*, 2010; Schlick-Steiner *et al.*, 2010; Dejaco *et al.*, 2016).

In this study, we used an integrative approach to delimit species of *Dicerapanorpa* using DNA barcoding, morphological comparison, geometric morphometric analysis and multilocus phylogenetic reconstruction. The main aims are as follows: (1) to clarify species diversity in *Dicerapanorpa*, especially in the *D. magna* group; (2) to resolve the boundaries between the morphologically similar species; and (3) to ascertain whether patterns of morphological clusters are congruent with molecular OTUs.

MATERIAL AND METHODS

SAMPLING

Specimens of *Dicerapanorpa* were collected throughout the Hengduan and Qinling-Bashan Mountains (Fig. 1) from 2009 to 2018. In total, 213 individuals of *Dicerapanorpa* and five specimens of outgroups from *Sinopanorpa* Cai & Hua in Cai *et al.*, 2008 and *Megapanorpa* Wang & Hua, 2019 were sequenced (Supporting Information, Table S1). In addition, using geometric morphometric analysis we examined 66 specimens of *D. magna* from the Qinling Mountains, 56 of *Dicerapanorpa minshana* from Minshan Mountain, 47 of *Dicerapanorpa hualongshana* from the Bashan Mountains, 20 of *Dicerapanorpa baiyunshana* Zhong & Hua, 2013 from Baiyunshan Mountain and 40 of *Dicerapanorpa shennongensis* Zhong & Hua, 2013 from Shennongjia. The specimens examined in this study are stored at –20 °C in 75 or 100% ethanol at the Entomological Museum, Northwest A&F University, China (NWAU).

LABORATORY PROCEDURES

Total genomic DNA was extracted from three legs removed from one side of each specimen, using a Genomic DNA Mini Preparation Kit with Spin Column (Beyotime, China). Four gene fragments (*COI*, *COII*, *cytb* and 28S rRNA) were amplified and sequenced. Primer sequences (Folmer *et al.*, 1994; Simon *et al.*, 1994; Whiting, 2002; Song & Liang, 2013) are shown in the Supporting Information (Table S2). Polymerase chain reaction products were sequenced bidirectionally at Shanghai Sangon Biotechnology Co. Ltd (China). All sequences were subsequently uploaded to BOLD
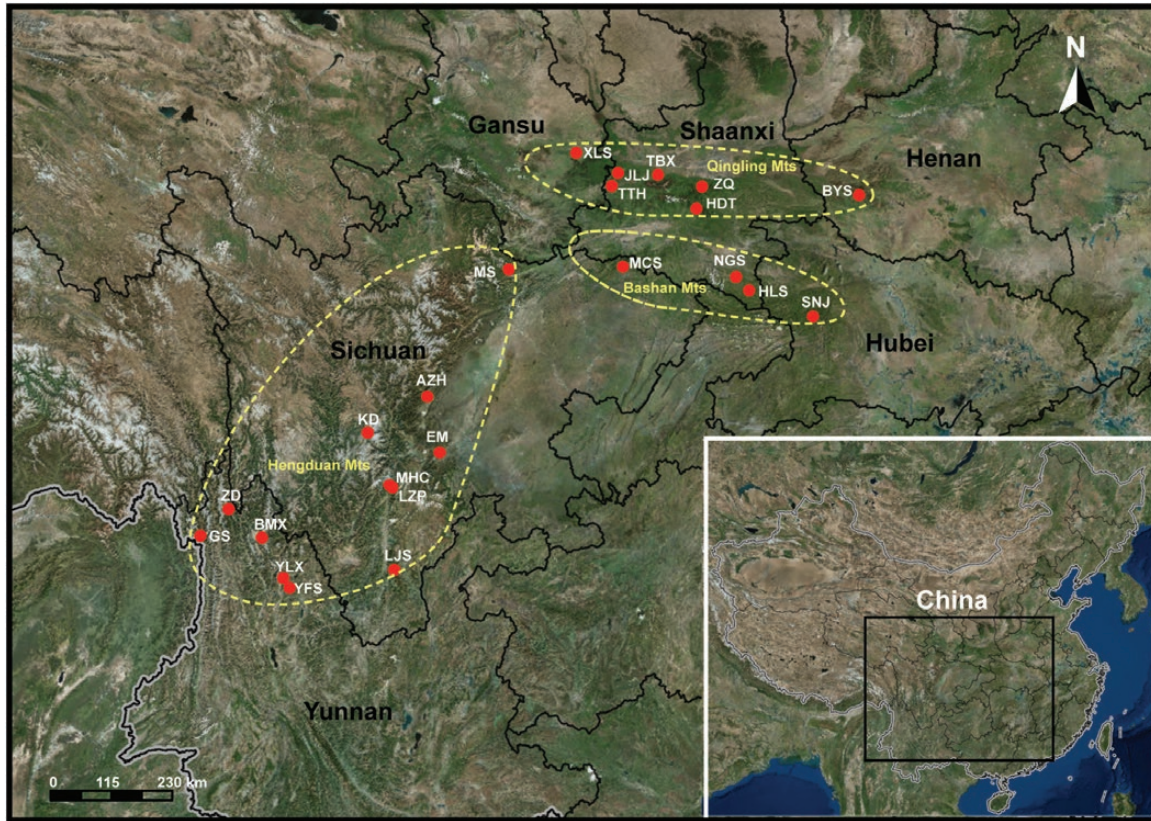
Figure 1. Collection localities for the *Dicerapanorpa* samples. Locality codes: AZH, Anzihe Nature Reserve, Sichuan; BMX, Baimaxueshan, Yunnan; BYS, Baiyunshan, Henan; EM, Mount Emei, Sichuan; GS, Gongshan, Yunnan; HDT, Huoditang, Shaanxi; HLS, Hualongshan, Shaanxi; JLJ, Jialingjiang, Shaanxi; KD, Kangding, Sichuan; LJS, Luojishan, Sichuan; LZP, Liziping Nature Reserve, Sichuan; MCS, Micangshan, Sichuan; MHC, Menghuocheng, Sichuan; MS, Minshan, Sichuan; NGS, Nangongshan, Shaanxi; SNJ, Shennongjia, Hubei; TBX, Taibaixian, Shaanxi; TTH, Tongtianhe Forest Park, Shaanxi; XLS, Xiaolongshan, Gansu; YFS, Yufengsi, Yunnan; YLX, Yulongxueshan, Yunnan; ZD, Zhongdian, Yunnan; ZQ, Zhuque Forest Park, Shaanxi.

(Ratnasingham & Hebert, 2007) together with the trace files and specimen information, and cross-referenced with GenBank (for detailed information, see Supporting Information, Table S1).

The DNA sequences were checked, assembled and edited with SeqMan (Swindell & Plasterer, 1997) or CodonCode Aligner v.6.0.2 (CodonCode Corporation, Dedham, MA, USA). Multiple sequence alignments were performed using MAFFT v.7.037 (Katoh *et al.*, 2009) with the accurate algorithm of G-INS-i. Ambiguous sites at both ends of the alignment were deleted manually using BioEdit v.7.0.9.0 (Hall, 1999).

DNA BARCODING

Barcode index number (BIN) assignments were generated in BOLD (Ratnasingham & Hebert, 2013) based on *COI* barcode sequences. Delimitation of OTUs was performed using the automatic barcode gap discovery (ABGD) method (Puillandre *et al.*, 2012a), generalized mixed

Yule coalescent (GMYC) procedure (Pons *et al.*, 2006; Fujisawa & Barraclough, 2013) and Bayesian Poisson tree processes (bPTP) (Zhang *et al.*, 2013).

Barcode index numbers

To assign DNA barcode sequences to a BIN, BOLD uses single linkage clustering with a threshold of 2.2%, followed by OTU refinement using Markov clustering (Ratnasingham & Hebert, 2013). All sequences were automatically assigned to a BIN in BOLD, and the BIN assignments are presented in the Supporting Information (Table S1).

Automated barcode gap discovery

The ABGD method generates clusters based on genetic distance distributions (Puillandre *et al.*, 2012a). The *COI* sequences ($N = 209$) were collapsed to haplotypes ($N = 118$) using ALTER (https://sing.

ei.uvigo.es/ALTER/) (Glez-Peña *et al.*, 2010). The haplotypes were uploaded on http://wwwabi.snv.jussieu.fr/public/abgd/abgdweb.html. The run was based on a Kimura 2-parameter distance matrix with a relative gap of one.

Generalized mixed Yule coalescent

The GMYC model-based likelihood analysis identifies the transition point between coalescent and speciation events (Pons *et al.*, 2006; Monaghan *et al.*, 2009) with a fully resolved ultrametric gene tree as input. The best-fitting substitution model (TrN+I+G) for *COI* was determined using jModelTest v.2.1.4 (Darriba *et al.*, 2012) based on the Bayesian information criterion. The Bayesian tree of *COI* haplotypes was reconstructed using BEAST v.1.8.0 (Drummond *et al.*, 2012) with an uncorrelated lognormal relaxed clock and a Yule speciation process. The analysis was run for 40 million generations, with a sample frequency of 1000. The convergence and stability were evaluated in Tracer v.1.5 (https://beast.bio.ed.ac.uk/software/tracer/), ensuring effective sample size > 200 for all parameters. A maximum clade credibility tree was assembled using TreeAnnotator v.1.8.0 (BEAST package), with the first 25% of samples removed as burn-in. The GMYC model was implemented in the R splits package using single- and multiple-threshold analyses, separately (available at http://r-forge.r-project.org/projects/splits).

Bayesian Poisson tree processes

A maximum likelihood (ML) tree of *COI* haplotypes was reconstructed using RAxML searches. The ML analysis was implemented in raxmlGUI v.1.31 (Silvestro & Michalak, 2012) with 1000 rapid bootstrap replicates and codon-specific partition scheme under the GTRCAT model. The bPTP analysis was carried out on the bPTP server (http://species.h-its.org/) with the ML tree as input (Zhang *et al.*, 2013). The OTUs recognized by these four methods were compared for congruence.

MORPHOLOGICAL COMPARISON

Female medigynia were dissected under a Nikon SMZ1500 stereoscopic zoom microscope, macerated in cold 5% NaOH for 3–5 min and rinsed in distilled water. The female medigynia were imaged digitally using a QImaging Retiga 2000R Fast 1394 Digital CCD camera attached to the microscope. Other photographs were taken using a Scientific Digital micrography system (ZEISS SteREO Discovery V20) equipped with an auto-montage imaging system (AxioCam IC).

The images were assembled using Adobe Photoshop CS4. Morphological characters, especially genital structures, were compared with the original images and descriptions (Carpenter, 1938; Cheng, 1957; Zhong & Hua, 2013a). Taxonomic assignments were attributed to OTUs based on the integrative criteria of morphological characters, geographical distribution and molecular clusters.

MORPHOMETRIC ANALYSES OF THE *D. MAGNA* GROUP

To evaluate species diversity in the *D. magna* group, we performed a geometric morphometric analysis based on female medigynia. The images were loaded into MakeFan7 (Sheets, 2009) with a comb of 20 lines to create a standardized template for landmark digitization. TPS files were generated for images using tpsUtil v.1.46 (Rohlf, 2010). To outline the exterior margin of a medigynium, 52 landmarks were digitized on each image using tpsDig2 v.2.19 (Rohlf, 2015). Generalized Procrustes analysis (GPA) was performed in CoordGen7a from the Integrated Morphometric Package (IMP) to eliminate the non-shape variation in size, location and orientation and generate Procrustes superimposition data (Sheets, 2012). Canonical variate analysis (CVA) was conducted on the shape data using CVAGen7b (Sheets, 2012). To test for differences in shape between species, a single-factor permutation multivariate analysis of variance (MANOVA) was performed using CVAGen7b with 1000 permutations. The variation in shape was visualized in MorphoJ v.1.05f (Klingenberg, 2011).

MOLECULAR PHYLOGENY

To reconstruct the phylogeny of *Dicerapanorpa*, *COI* sequences were concatenated with those for *COII*, *cytb* and 28S rRNA. Phylogenetic reconstruction was conducted using ML analysis and Bayesian inference (BI). The most suitable substitution model and partition scheme were determined for the combined dataset using PartitionFinder v.1.1.1 (Lanfear *et al.*, 2012). They are as follows: TrN+I+G for the first codon position of *COI*, *COII* and *cytb*, HKY+I+G for the second codon position, TIM+I+G for the third codon position, and K80 for 28S rRNA.

Maximum likelihood analysis was executed in raxmlGUI v.1.31 (Silvestro & Michalak, 2012) with codon-specific partition under the GTRCAT model. Bootstrap values (BVs) were calculated with 1000 rapid bootstrap replicates. Bayesian inference was performed in MrBayes v.3.2.6 (Ronquist & Huelsenbeck, 2003) through the CIPRES Science Gateway (Miller *et al.*, 2010). Two independent runs

with four Markov chain Monte Carlo chains were performed for 40 million generations, with sampling every 1000 generations. The average standard deviation of split frequency < 0.01 indicates that the sampling of posterior distribution was adequate. The stationarity was evaluated with Tracer v.1.5 (http://beast.bio.ed.ac.uk/software/tracer/) by plotting log-likelihood values vs. generation number. The first 25% of the samples were discarded as burn-in, and the remaining trees were used to generate a majority consensus tree and estimate the posterior probabilities (PPs) in TreeAnnotator v.1.8.4 (BEAST package). The tree was visualized in FigTree v.1.3.1 (http://beast.bio.ed.ac.uk/figtree).

RESULTS

DNA BARCODING

BOLD assigned 214 *COI* sequences of *Dicerapanorpa* to 12 BINs (Fig. 2). With the ABGD method, after two extreme prior divergences were excluded, the remaining prior intraspecific distances resulted in the recognition of ten, 11 and 23 partitions. The molecular OTU count (23) was much more biologically realistic at the prior of 0.00167 in the recursive analysis. GMYC analysis is susceptible to oversplitting species, and the multiple-threshold model fragmented most morphological species into several individual clusters. Therefore, we preferred the OTU count of 26 from the single-threshold model. In contrast, the bPTP analysis produced 18 clusters with the highest Bayesian solution. Taking morphological uniqueness into consideration, we determined a final OTU count of 19.

The *COI* haplotype tree resolved four robust clades (I–IV in Fig. 2) of *Dicerapanorpa*. In clade I, BIN, ABGD and GMYC clustered all samples from Anzihe Nature Reserve, Sichuan and Mount Emei, Sichuan into three OTUs (1a, 1b and 2), whereas bPTP merged these OTUs into a single cluster. In clade II, ABGD and GMYC generated four OTUs (4–7), whereas BIN grouped OTU6 and OTU7 together, and bPTP split OTU6 into two clusters. In clade III, BIN and bPTP recognized four OTUs (8–11), whereas ABGD and GMYC delineated five OTUs, splitting OTU10 into two partitions. The main discordance of these four approaches involved clade IV (i.e. the *D. magna* group). BIN produced only one cluster in clade IV, whereas ABGD and GMYC oversplit the samples, and the bPTP result was the most biologically realistic, with members from Shennongjia, Hubei split into three OTUs (15a–15c).

MORPHOLOGICAL COMPARISON

Species assignments were based primarily on overall morphological features, including the anal horn (Fig. 3), notal organ (Fig. 4), male genitalia (Fig. 5) and female medigynium (Fig. 6). Through integrative analyses of morphological characters, molecular clusters and geographical information, we recognized three new species (*D. lativalva*, *D. minshana* and *D. hualongshana*), which are described below. In general, morphological species corresponded well to OTUs, but several discordances existed between molecular and morphological clusters. For example, the allopatric *Dicerapanorpa yijunae* Hu & Hua, 2019 and *Dicerapanorpa kimminsi* (Carpenter, 1948) possess morphologically distinct male genitalia (Fig. 5A, B) and female medigynia (Fig. 6A, B), but lack molecular divergence (OTU1a, OTU1b and OTU2 in Fig. 2). The specimens of *D. shennongensis* with the same locality and conserved body, wing coloration and pattern are clustered into three OTUs (15a–15c in Fig. 2), but exhibit morphological diversity in the female medigynium (Fig. 6Q–S).

GEOMETRIC MORPHOMETRIC ANALYSES

The CVA indicated that *D. minshana* and *D. hualongshana* were clearly separated from each other and from *D. magna*, *D. baiyunshana* and *D. shennongensis* (Fig. 7A). The sole cases of overlap involved *D. baiyunshana* and *D. shennongensis*. The permutation MANOVA confirmed significant shape differences in female medigynia of these five species in the *D. magna* group [$F(4, 224) = 71.780, P < 0.001$]. The CVA discriminated them based on female medigynia (axis 1, $\lambda = 0.003$, $\chi^2 = 1415.174$, d.f. = 400, $P < 0.001$; axis 2, $\lambda = 0.006$, $\chi^2 = 913.085$, d.f. = 297, $P < 0.001$; axis 3, $\lambda = 0.068$, $\chi^2 = 469.587$, d.f. = 196, $P < 0.001$; axis 4, $\lambda = 0.334$, $\chi^2 = 192.613$, d.f. = 97, $P < 0.001$). The first two canonical variates (CV1 and CV2) accounted for 48.69 and 34.06% of the total shape variation, respectively. The shape variables related to CV1 were a greatly elongated axis, slightly lowered posterior arms and expanded upper sides, whereas the shape variables involved in CV2 were the rapidly constricted middle sides and expanded lower sides (Fig. 7B).

MOLECULAR PHYLOGENY

This study recovered 214 sequences of *COI*, 189 of *COII*, 198 of *cytb* and 166 of 28S rRNA. After alignment and the deletion of ambiguous sites, *COI* had a size range of 777 bp, *COII* of 699 bp, *cytb* of 567 bp and 28S rRNA

Figure 2. Bayesian inference tree for *Dicerapanorpa* spp. based on mitochondrial *COI* haplotypes. Posterior probabilities are shown on the nodes. The right vertical bars indicate molecular partitions and final operational taxonomic units (OTUs) from delimitation analyses. Morphological species are uniquely coloured.
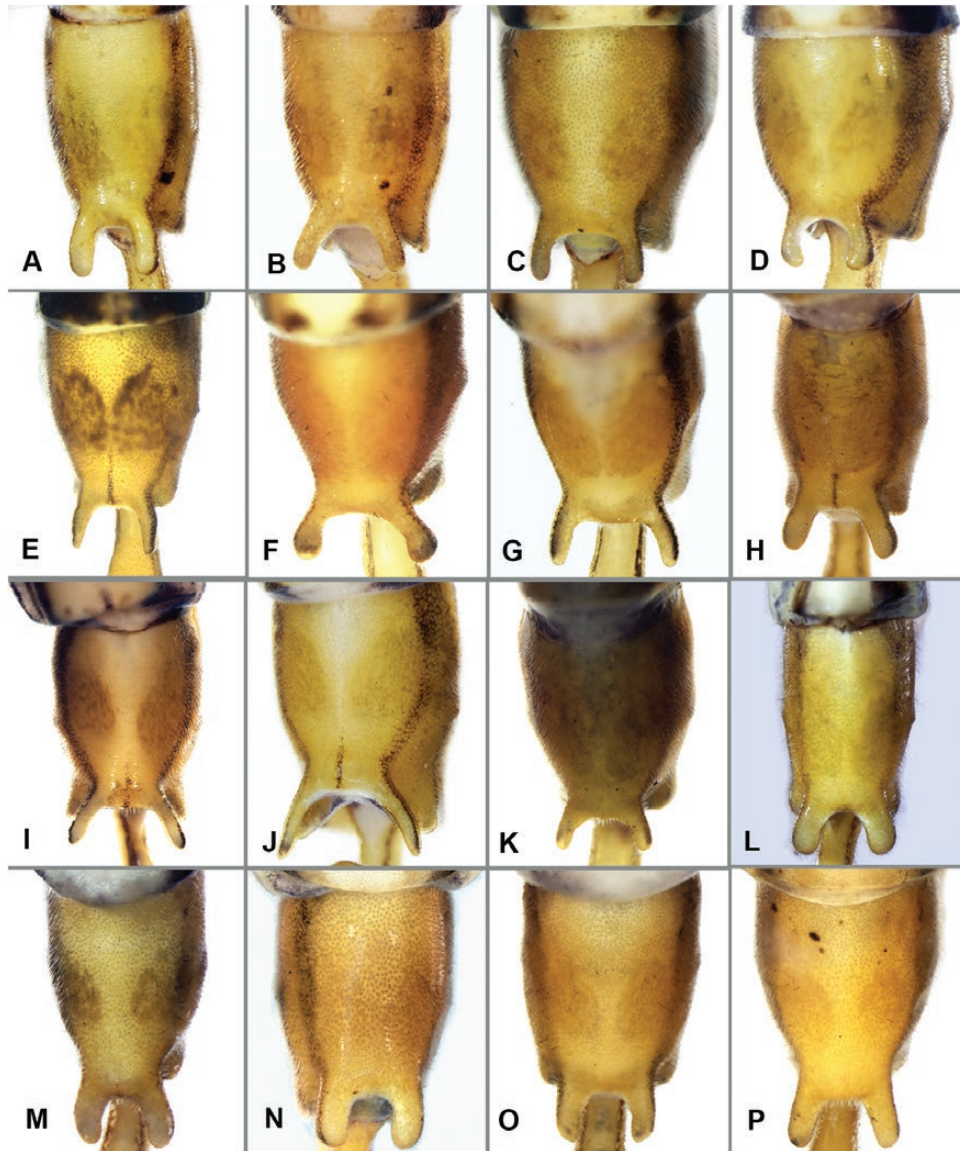
Figure 3. Anal horns for 16 species of *Dicerapanorpa*: A, *D. yijunae*; B, *D. kimminsi*; C, *D. diceras*; D, *D. lativalva*; E, *D. zhongdianensis*; F, *D. luojishana*; G, *D. tanae*; H, *D. macula*; I, *D. deqenensis*; J, *D. tjederi*; K, *D. tenuis*; L, *D. minshana*; M, *D. hualongshana*; N, *D. magna*; O, *D. shennongensis*; P, *D. baiyunshana*.

of 851 bp. In total, 197 individuals with at least three loci were selected for the phylogenetic reconstruction.

The BI (Fig. 8) and ML trees (Fig. 9) reveal four identical monophyletic clades (I–IV) of *Dicerapanorpa*, as mentioned above (Fig. 2). The monophyly of most species was strongly supported, with a few exceptions. In clade I, *D. lativalva* was well supported to be monophyletic, whereas *D. yijunae* and *D. kimminsi* were paraphyletic. The samples of *D. yijunae* and *D. kimminsi* were mixed, forming a sister group to *D. lativalva* (PP = 1, BV = 99). In clade II, *D. zhongdianensis*, *D. deqenensis* Hu, Wang & Hua, 2019 and *D. macula* were strongly supported as

monophyletic clades. *Dicerapanorpa deqenensis* was the sister species to *D. macula*, but the phylogenetic positions of *D. zhongdianensis* and *Dicerapanorpa tjederi* (Carpenter, 1938) were inconsistent between the BI and ML trees. In clade III, all the species (*Dicerapanorpa tanae* Hu, Wang & Hua, 2019, *Dicerapanorpa tenuis* Hu, Wang & Hua, 2019, *Dicerapanorpa luojishana* Hu & Hua, 2019 and *D. diceras*) were well supported as monophyletic in the BI tree (Fig. 8), whereas *D. luojishana* was paraphyletic with *D. diceras* in the ML tree (Fig. 9). The phylogenetic positions of *D. tanae* and *D. tenuis* were uncertain because of the inconsistent topology in both
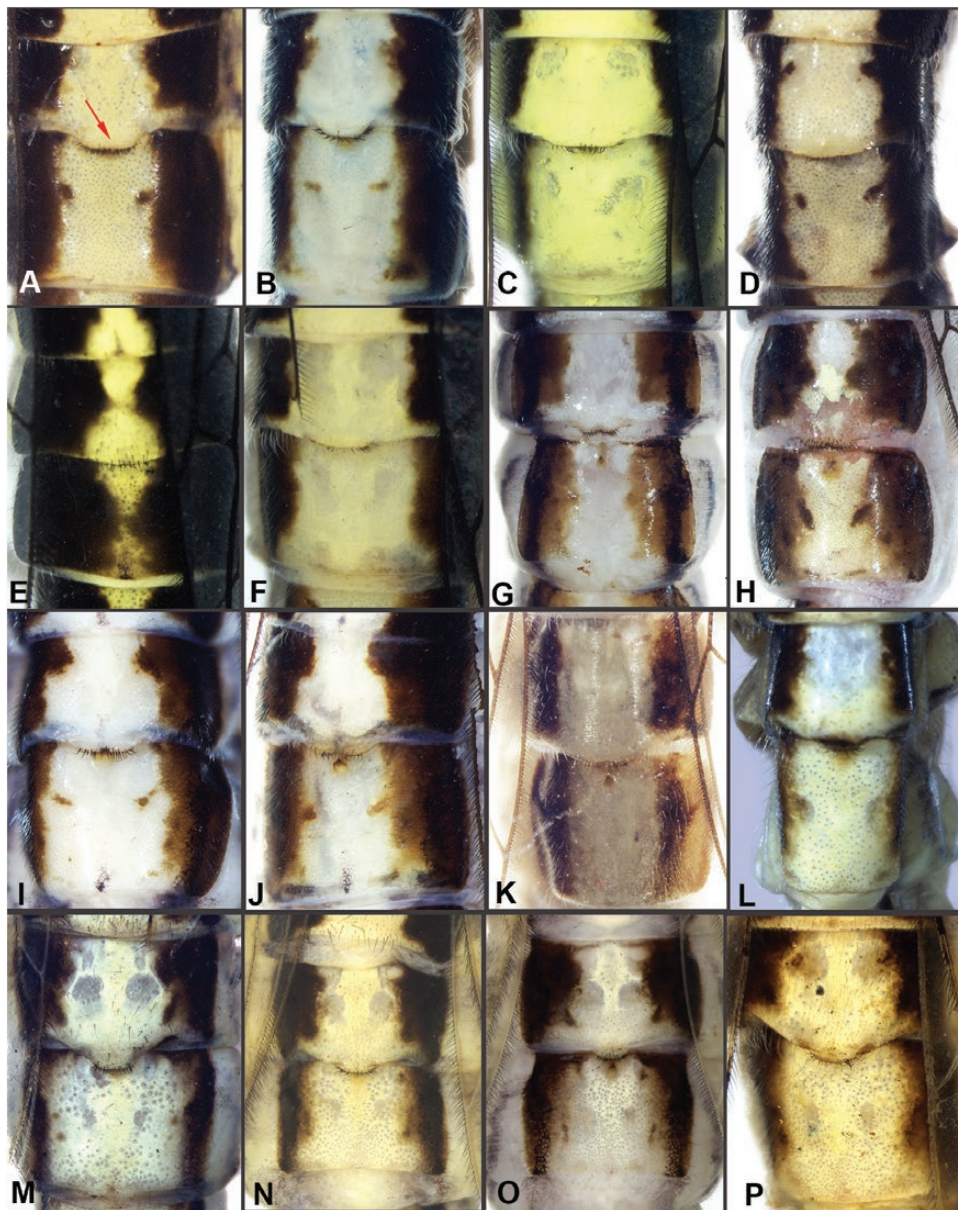
Figure 4. Notal organs for 16 species of *Dicerapanorpa*: A, *D. yijunae*; B, *D. kimminsi*; C, *D. diceras*; D, *D. lativalva*; E, *D. zhongdianensis*; F, *D. luojishana*; G, *D. tanae*; H, *D. macula*; I, *D. deqenensis*; J, *D. tjederi*; K, *D. tenuis*; L, *D. minshana*; M, *D. hualongshana*; N, *D. magna*; O, *D. shennongensis*; P, *D. baiyunshana*.

trees. Clade IV was separated into two subclades with high support values (PP = 1, BV = 100). One subclade included *D. shennongensis* and *D. baiyunshana*, with *D. shennongensis* paraphyletic with *D. baiyunshana*. The other subclade included *D. minshana*, *D. hualongshana* and *D. magna*. *Dicerapanorpa minshana* was the sister species to *D. magna*, with both forming the sister group to *D. hualongshana* in the BI tree. However, the relationships among these three species were not well resolved in the ML tree.

TAXONOMY

DICERAPANORPA LATIVALVA HU & HUA SP. NOV.

(FIGS 3D, 4D, 5D, 6C, 10, 11)

lsid:zoobank.org:act:D8E5BA1A-D5FF-4F79-B543-E3D5AB367B6B

Type material

Holotype: CHINA: ♂, Menghuocheng (29.00°N, 102.30°E), 2600 m, Shimian County, Sichuan, 26 July 2016, leg. Lu Jiang.
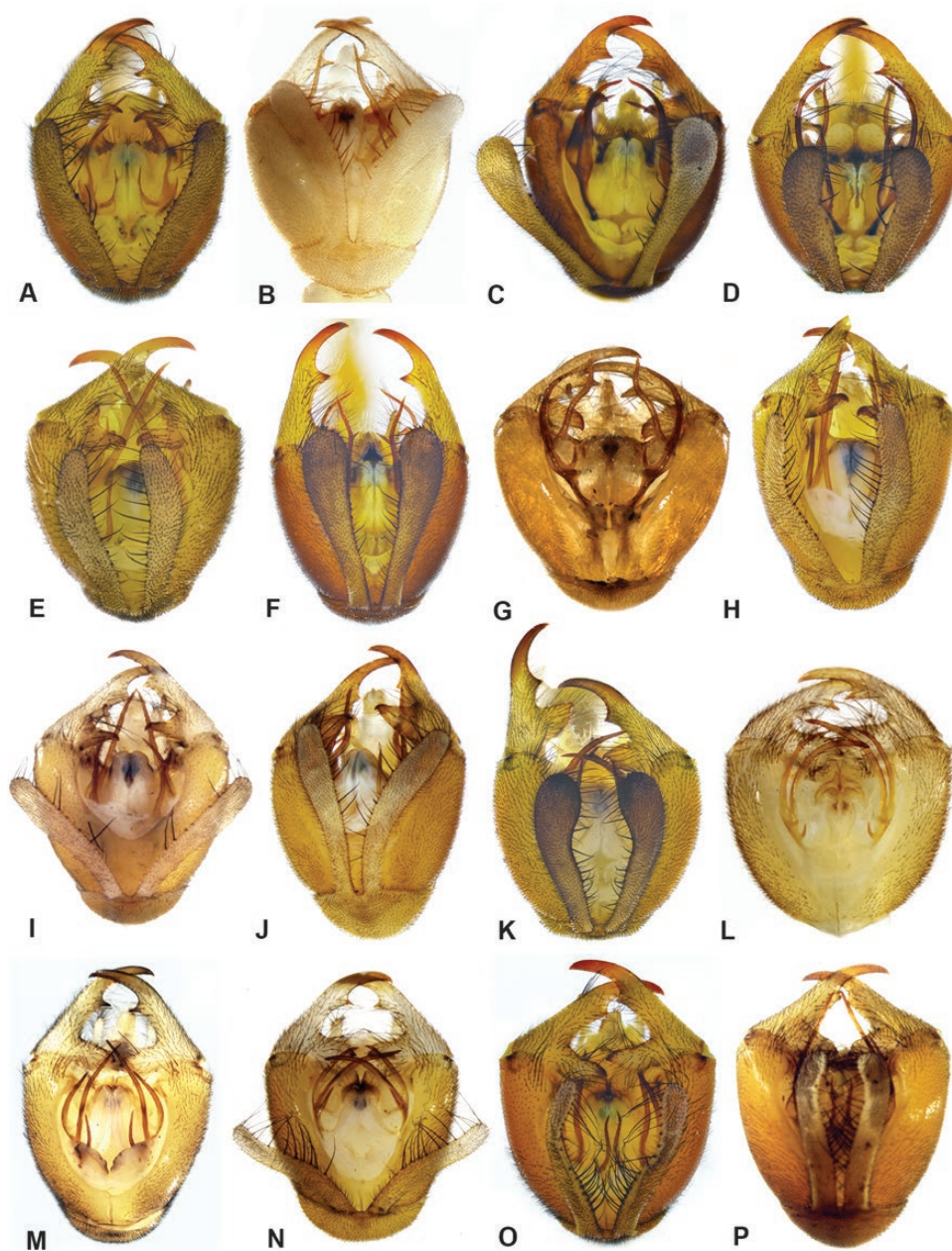
Figure 5. Male genitalia for 16 species of *Dicerapanorpa*: A, *D. yijunae*; B, *D. kimminsi*; C, *D. diceras*; D, *D. lativalva*; E, *D. zhongdianensis*; F, *D. luojishana*; G, *D. tanae*; H, *D. macula*; I, *D. deqenensis*; J, *D. tjederi*; K, *D. tenuis*; L, *D. minshana*; M, *D. hualongshana*; N, *D. magna*; O, *D. shennongensis*; P, *D. baiyunshana*.

Paratypes: Six ♂, five ♀, Menghuocheng and Liziping Nature Reserve, Shimian County, Sichuan, 22–26 July 2016, leg. Lu Jiang.

Etymology

The specific epithet is composed of the Latin *latus*, wide or broad, and *valvae*, valves or doors, referring to the broad dorsal valves of the male aedeagus.

Diagnosis

The new species resembles *D. diceras*, but can be distinguished from the latter by the following characters: (1) basal branch of male paramere slender and straight (cf. broadened basally); (2) lateral branches semicircular at basal two-thirds and parallel at distal one-third (cf. curved inward); (3) dorsal valve of male aedeagus broad, reaching
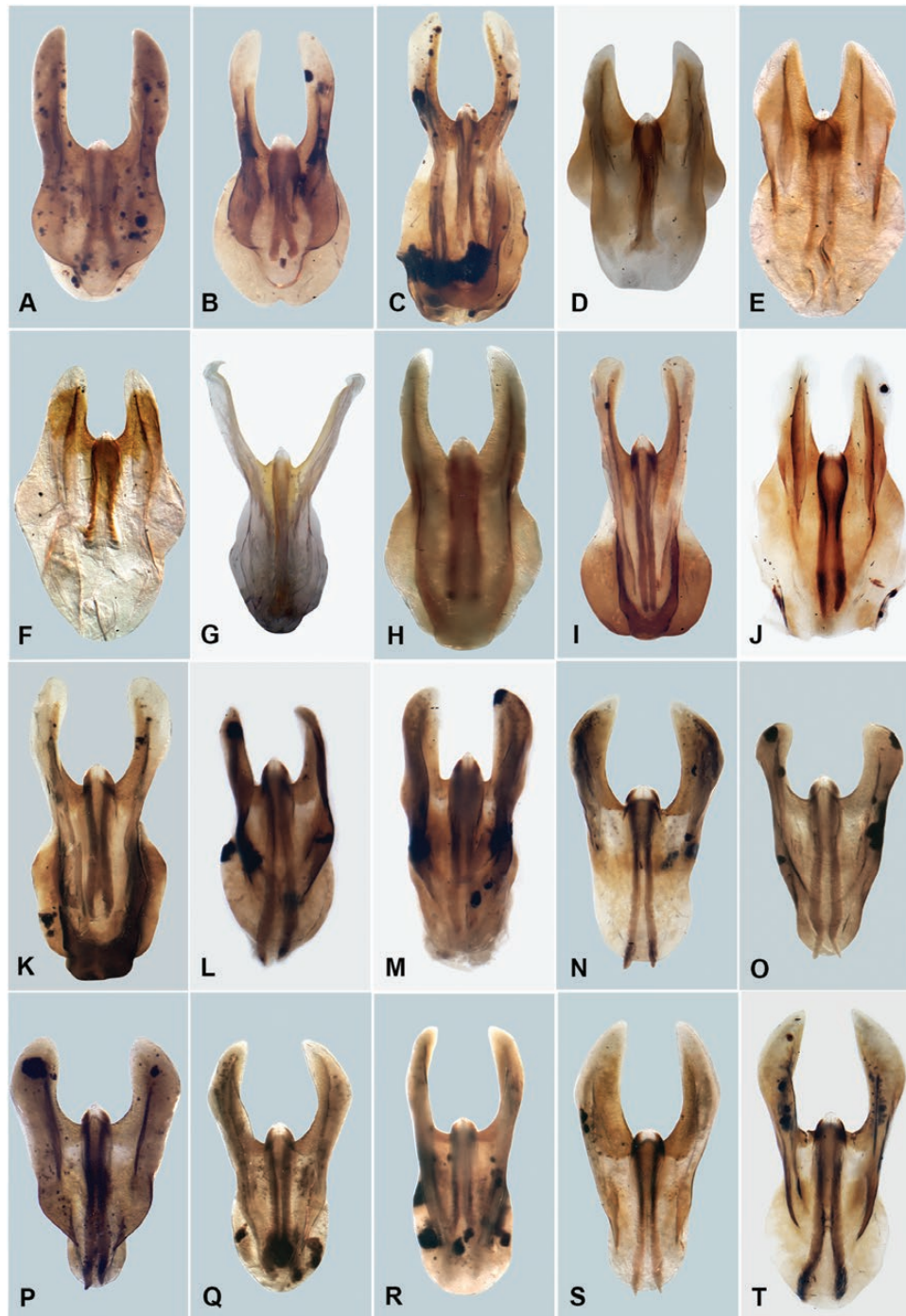
Figure 6. Female medigynium for 16 species of *Dicerapanorpa*: A, *D. yijunae*; B, *D. kimminsi*; C, *D. lativalva*; D, *D. deqenensis*; E, *D. macula*; F, *D. zhongdianensis*; G, *D. tenuis*; H, *D. tanae*; I, *D. luojishana*; J, *D. tjederi*; K, *D. diceras*; L, M, *D. minshana*; N, *D. hualongshana*; O, P, *D. magna*; Q–S, *D. shennongensis*; T, *D. baiyunshana*.

basal process of gonostylus (cf. slender, short); and (4) main plate of female medigynium pear-shaped (cf. rounded).

Description

Head: Head yellow. Vertex pale yellow. Ocellar triangle black. Rostrum yellow with two black
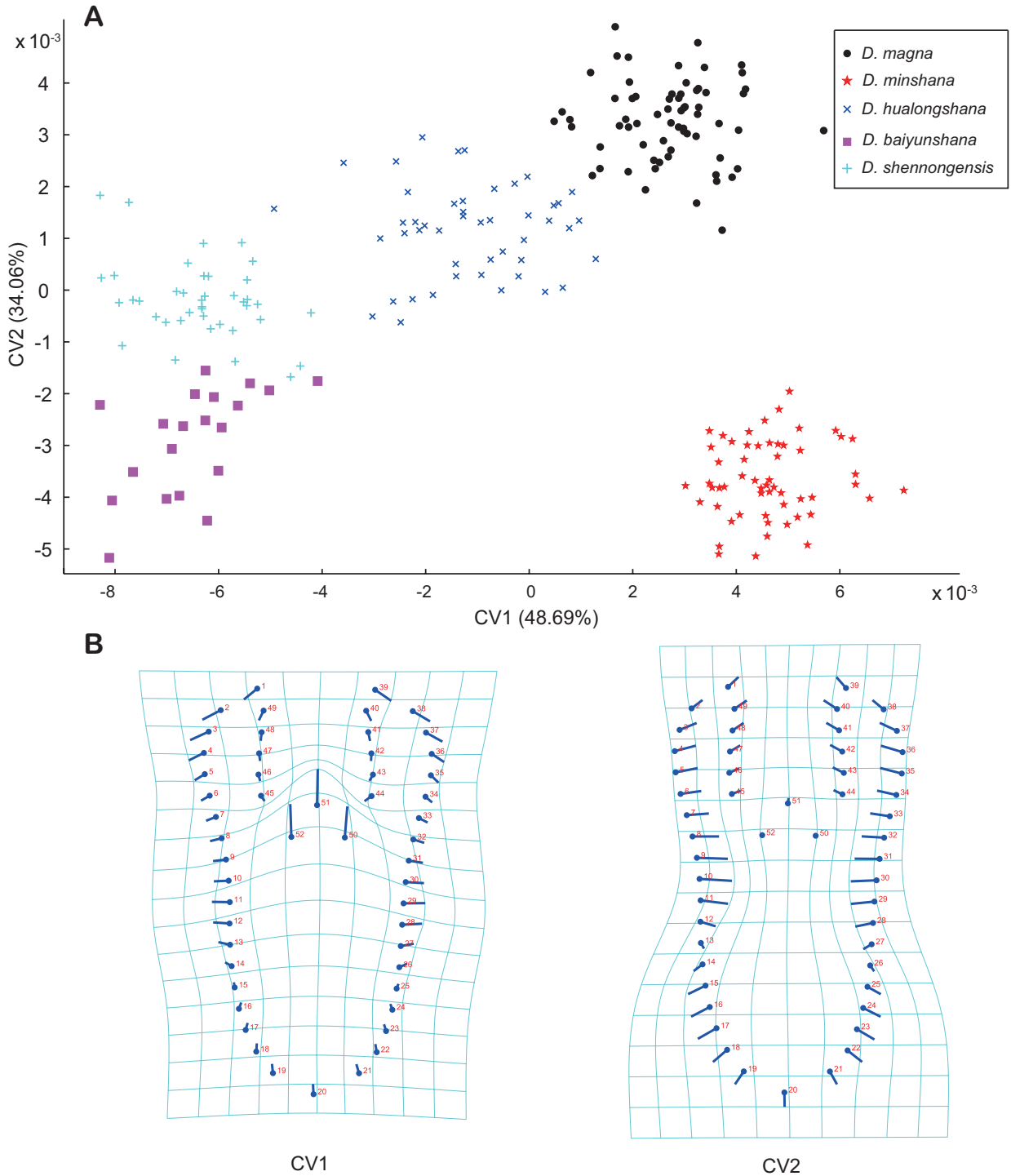
Figure 7. Canonical variate analysis of the shape variables based on female medigynia of *Dicerapanorpa magna*, *D. minshana*, *D. hualongshana*, *D. baiyunshana* and *D. shennongensis*. A, scatter plots of canonical variates CV1 vs. CV2 are shown for different species. B, shape variations along CV1 and CV2 illustrated by deformation grid graphs.
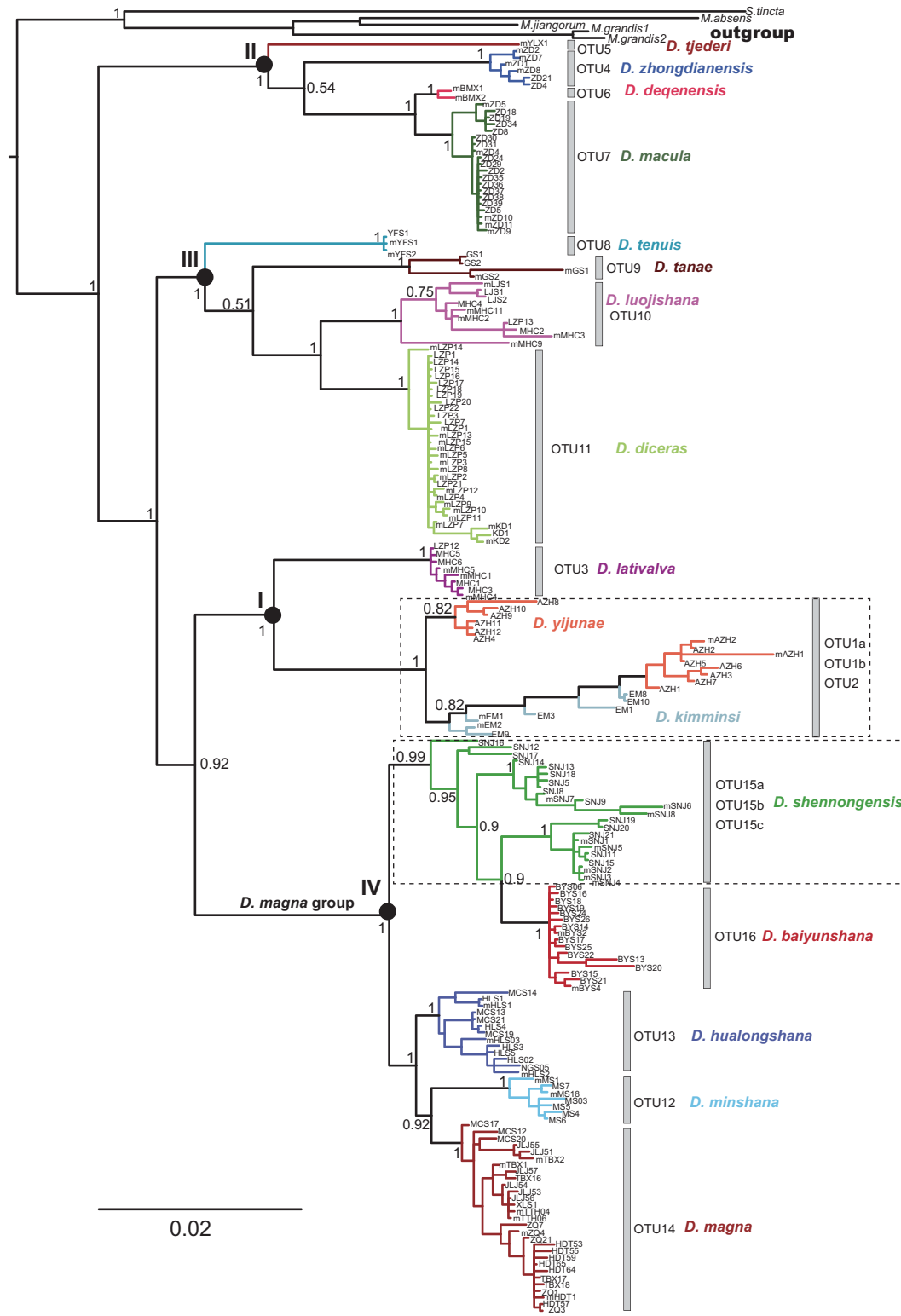
Figure 8. Majority consensus tree obtained via Bayesian inference for *Dicerapanorpa* spp. based on the concatenated *COI*, *COII*, *cytb* and 28S rRNA dataset. Posterior probabilities are shown on the nodes. Morphological species are uniquely coloured.
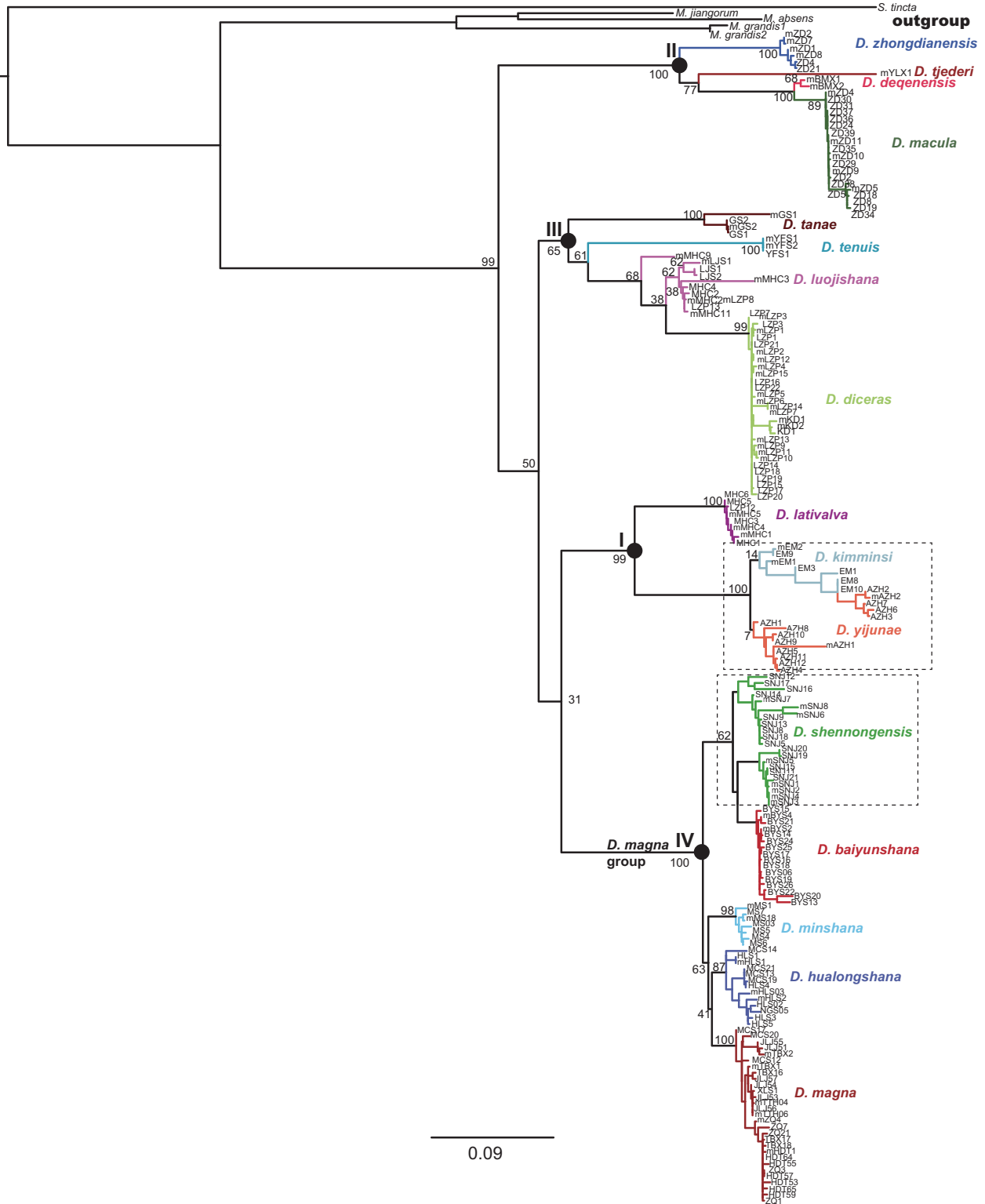
Figure 9. Maximum likelihood tree for *Dicerapanorpa* spp. based on the concatenated dataset of *COI*, *COII*, *cytb* and 28S rRNA. Bootstrap values are shown on the nodes.

lateral longitudinal stripes. Antenna blackish brown (Figs 10, 11A, B).

Thorax: Pronotum yellow, with long black setae along anterior margin and a black longitudinal stripe along each side. Meso- and metanotum yellow, with two black longitudinal stripes laterally. Pleura yellow. Legs cream coloured, with tarsomeres blackish (Figs 10, 11A, B).

Wings: Male holotype: forewing length 14.6 mm, width 3.7 mm; hindwing length 13.9 mm, width 3.5 mm; wing membrane hyaline, without distinct markings (Fig. 11A). Female: forewing length 15.4–16.6 mm, width 3.8–4.1 mm; hindwing length 14.2–15.2 mm, width 3.8–4.1 mm; similar to male in general appearance (Figs 10B, 11B).

Abdomen: Terga I–V (T1–T5) yellowish, with two black longitudinal lateral stripes; sterna and pleura yellow (Figs 10, 11). Male: notal organ of T3 slightly prominent, bearing black setae posteriorly (Fig. 4D); T6 yellowish brown, with a pair of anal horns on posterior margin (Figs 3D, 11A); abdominal segments VII and III (A7–A8) brownish yellow, elongate, constricted at basal half and thickened at apical half, but A8 much
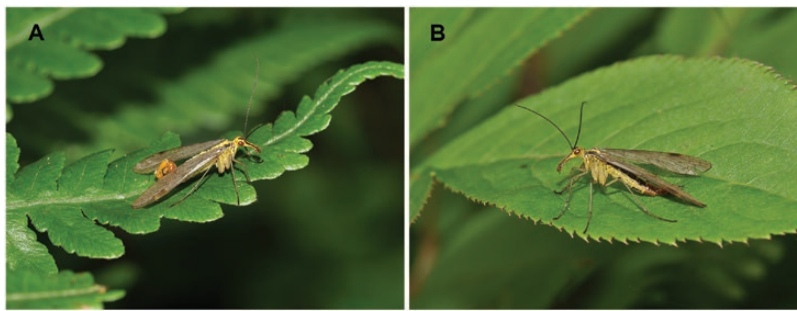
Figure 10. Habitus of *Dicerapanorpa lativalva*: A, male; B, female.

Figure 11. *Dicerapanorpa lativalva*: A, male holotype, dorsal view; B, female paratype, dorsal view; C, D, male genital bulb, dorsal and ventral views, respectively; E, female subgenital plate, ventral view; F, female medigynium, ventral view. Abbreviations: ae, aedeagus; ax, axis; bb, basal branch; bp, basal process; ep, epandrium; gcx, gonocoxite; gs, gonostylus; hv, hypovalve; lb, lateral branch; mb, mesal branch; mp, main plate; mt, median tooth; pa, posterior arm; sgp, subgenital plate. Scale bars: 5.0 mm (A, B); 0.5 mm (C, D); 0.1 mm (E, F).

thinner than A7 distally. Female: abdominal segments gradually narrowed distally (Figs 10B, 11B).

Male genitalia: Genital bulb spherical, yellowish brown. Epandrium broad basally and narrowed distally, terminating with a shallow, broad, U-shaped emargination, extending over apex of gonocoxite (Fig. 11C). Hypovalve greatly broadened toward apex and slightly curved inward distally, bearing long bristles along inner margin (Figs 5D, 11D). Gonostylus smoothly curved, bearing a developed basal process and a sharp median tooth along inner margin. Parameres trifurcate: basal branches slender and straight, nearly parallel, reaching basal process of gonostylus; mesal branches divergent at base and convergent at apex, reaching median tooth of gonostylus; lateral branches semicircular at basal two-thirds and parallel at distal one-third. Ventral valves of aedeagus membranous and slender, reaching apex of gonocoxite; dorsal valves broadened and elongate, reaching basal process of gonostylus.

Female genitalia: Subgenital plate broad, trapezoidal, terminating in a ligulate process (Fig. 11E). Medigynium elongate and pear-shaped, folded ventrally on each side. Main plate nearly rectangular, twice as long as posterior arms. Axis concealed in main plate, slightly protruding at apex (Figs 6C, 11F).

DICERAPANORPA HUALONGSHANA HU & HUA SP. NOV.

(FIGS 3M, 4M, 5M, 6N, 12, 13)

lsid:zoobank.org:act:81200120-41F3-43F6-94B2-AD9AA32EA0FD

Type material

Holotype: CHINA: ♂, Hualongshan Mountain (32.01°N, 109.36°E), 2100 m, Pingli County, Shaanxi, 12 July 2015, leg. Bao-Zhen Hua.

Paratypes: Seven ♀, Mount Nangongshan (32.29°N, 109.06°E), Langao County, Shaanxi, 11 June 2013, leg. Jing Chen and Qin-Xiao Chen; Five ♂, three ♀, Hualongshan Mountain, Pingli County, Shaanxi, 24 June 2018, leg. Kai Gao, Yuan Hua and Yu-Ru Yang; one ♂, 21 ♀, Mount Nangongshan, Langao County, Shaanxi, 26 June 2018, leg. Yuan Hua and Kai Gao; four ♂, ten ♀, Chengkou County (31.84°N, 109.107°E), Chongqing, 20 June 2018, leg. Kai Gao.

Etymology

The specific epithet refers to the type locality, Hualongshan Mountain.

Diagnosis

This new species resembles *D. shennongensis*, but can be readily differentiated from the latter by the following characters: (1) mesal branches of male parameres convergent distally (cf. parallel); and (2) main plate of female medigynium broad, posterior arms short (cf. slender and long).

Description

Head: Head mostly yellow. Vertex yellowish. Ocellar triangle black. Rostrum yellow, without distinct black longitudinal stripes. Antenna blackish brown (Fig. 12A, B).

Thorax: Pro-, meso- and metanotum yellowish, bearing black stout setae anteriorly and two black longitudinal stripes laterally. Pleura pale yellow. Legs yellowish brown (Fig. 12A, B).

Wings: Male holotype: forewing length 15.8 mm, width 4.2 mm, yellowish with dark brown markings; apical band enclosing a large hyaline window; pterostigmal band with a broad basal branch and a reduced separated distal branch; basal band extremely reduced; marginal and basal spots indistinct; hindwing length 13.9 mm, width 4.0 mm, with more degenerated markings (Fig. 12A). Female: forewing length 14.8–17.2 mm, width 4.0–4.9 mm, basal band reduced, extending from vein R_1 to 1A; pterostigma and apical bands complete; marginal spot extending from vein R_1 to R_{4+5}. Hindwing length 13.8–16.1 mm, width 4.0–4.8 mm, similar to forewing in general appearance (Fig. 12B).

Abdomen: T1–T5 pale yellow, with two black longitudinal stripes laterally (Fig. 12A, B). Male: notal organ of T3 well developed, bearing thick setae on posterior margin (Fig. 4M); T6 yellowish brown, with a pair of digitate anal horns posteriorly (Fig. 3M); abdominal segment VII (A7) yellowish brown, elongate, constricted basally and abruptly dilated distally; A8 similar to A7, but much thinner apically (Fig. 12A). Female: abdominal segments gradually narrowed distally (Fig. 12B).

Male genitalia: Genital bulb yellowish brown, elliptic. Epandrium broad at base, gradually narrowing toward apex, with a deep U-shaped terminal emargination (Fig. 12C). Hypovalve not reaching apex of gonocoxite, with long bristles along inner margin (Figs 12D, 13C). Gonostylus shorter than gonocoxite, with a developed pentagon-shaped basal process and a small, sharp median tooth (Fig. 12C, D). Parameres trifurcate: basal branches short, nearly parallel; mesal branch elongate, curved inward at apex, reaching basal process of gonostylus; lateral branch incurved, reaching or
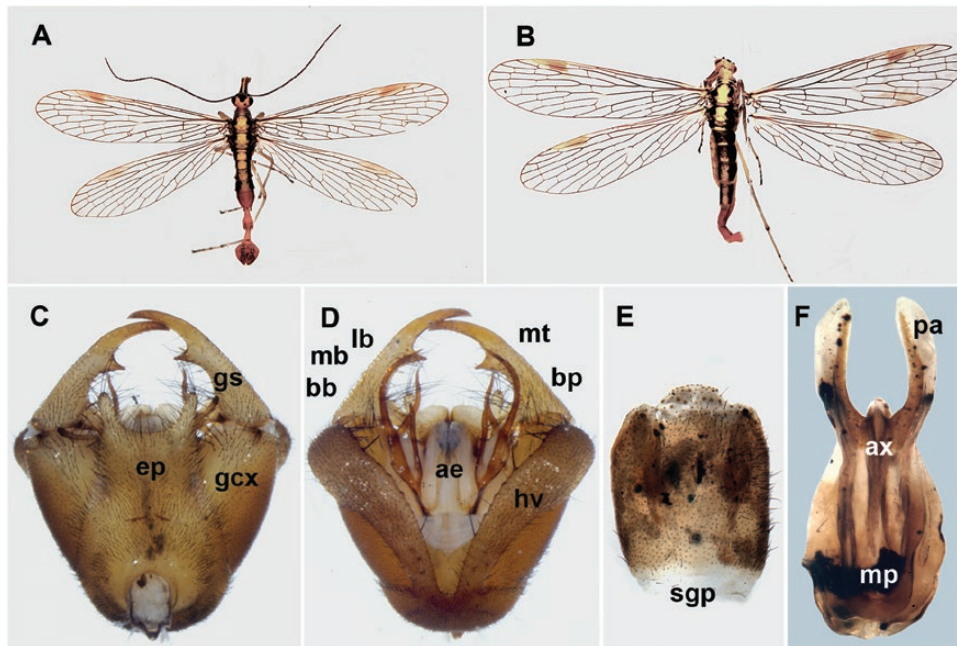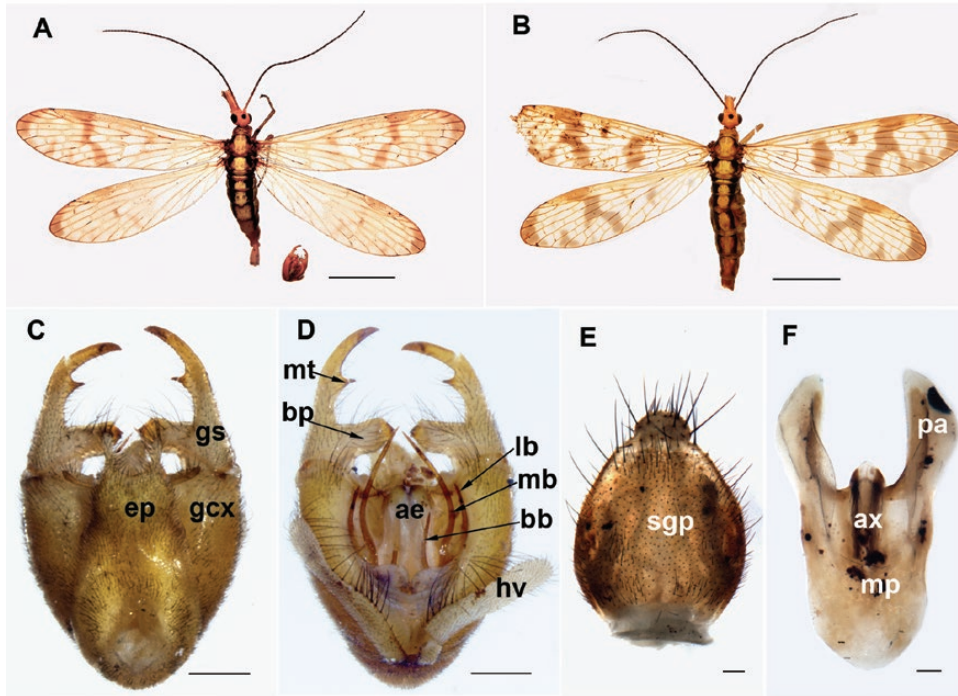
Figure 12. *Dicerapanorpa hualongshana*: A, male holotype, dorsal view; B, female paratype, dorsal view; C, D, male genital bulb, dorsal and ventral views, respectively; E, female subgenital plate, ventral view; F, female medigynium, ventral view. Abbreviations: ae, aedeagus; ax, axis; bb, basal branch; bp, basal process; ep, epandrium; gcx, gonocoxite; gs, gonostylus; hv, hypovalve; lb, lateral branch; mb, mesal branch; mp, main plate; mt, median tooth; pa, posterior arm; sgp, subgenital plate. Scale bars: 5.0 mm (A, B); 0.5 mm (C, D); 0.1 mm (E, F).
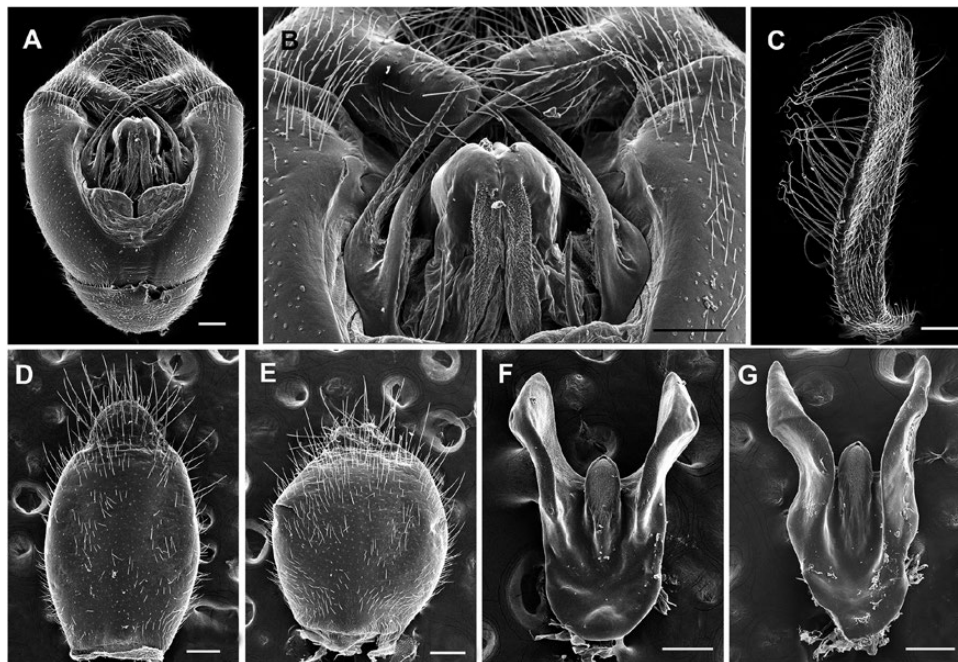

Figure 13. Scanning electron micrographs of male (A–C) and female genitalia (D–G) of *Dicerapanorpa hualongshana*: A, male genital bulb, with hypandrium removed, ventral view; B, magnification of A to show the male aedeagus, ventral view; C, right hypovalve, ventral view; D, E, female subgenital plate; F, G, medigynium. Scale bars: 0.2 mm.

exceeding apex of ventral valve. Ventral valves of aedeagus long, slender; dorsal valves sclerotized, not reaching apex of gonocoxite (Fig. 12D).

Female genitalia: Subgenital plate ovoid, terminating in a ligulate process, covered with long bristles caudally (Fig. 12E). Main plate of female medigynium broad, nearly rectangular (Fig. 12F). Posterior arms shorter than main plate. Axis concealed in main plate, slightly protruding beyond main plate at apex.

Remarks

Different individuals of this species exhibit variations in male aedeagus, paramere (Figs 4M, 13A, B), female subgenital plate (Fig. 13D, E) and medigynium (Figs 6N, 13F, G).

DICERAPANORPA MINSHANA Hu & Hua sp. nov.

(Figs 3L, 4L, 5L, 6L, M, 14, 15)
lsid:zoobank.org:act:B0F01DAE-2C1F-473E-B324-862C92D1D86A

Type material

Holotype: CHINA: ♂, Laohegou Nature Reserve (32.47°N, 104.73°E), Minshan Mountain, 1800 m, Pingwu County, Sichuan, 6 May 2013, leg. Shuang Xue.

Paratypes: Thirteen ♂, three ♀, same data as holotype; 13 ♂, 16 ♀, same locality as holotype, 28 May 2018, leg. Kai Gao.

Etymology

The specific epithet refers to the type locality, Minshan Mountain.

Diagnosis

This new species can be differentiated readily from *D. magna* by the following characters: (1) male genital bulb spherical (cf. long and elliptical); (2) basal branch of male paramere short, hook-shaped (cf. relatively long); and (3) main plate of female medigynium nearly rectangular distally, constricted mesally and smoothly curved basally (cf. subtriangular or constricted rapidly at base).

Description

Head: Head yellow. Vertex yellowish. Ocellar triangle black. Antenna blackish brown. Rostrum yellowish, without black lateral longitudinal stripes (Fig. 14A, B).

Thorax: Pro-, meso- and metanotum yellow, bearing several setae anteriorly and two black longitudinal stripes laterally. Pleura light yellow. Legs yellowish brown, with tarsomeres gradually darkened toward apex (Fig. 14A, B).

Wings: Male holotype: forewing length 16.5 mm, width 4.5 mm, yellowish, apical band reduced; pterostigma band incomplete and dark brown, with reduced basal and distal branches; basal band extending from vein R_s to CuP, other markings indistinct; hindwing length 15.2 mm, width 4.3 mm, similar to forewing, but with more degenerated markings (Fig. 14A). Female: forewing length 15.5–17.6 mm, width 4.1–4.9 mm; hindwing length 14.1–16.4 mm, width 4.0–4.7 mm; similar to male in general appearance (Fig. 14B).

Abdomen: T1–T5 yellowish, with two black lateral longitudinal stripes (Fig. 14A, B). Male: notal organ developed, covered with numerous black setae posteriorly (Fig. 4L); T6 brownish yellow, bearing a pair of digitate anal horns posteriorly (Figs 3L, 14A); A7 and A8 yellowish brown, elongate, constricted at basal half and dilated at distal half, but A8 much thinner than A7 distally (Fig. 14A). Female: abdominal segments gradually narrowed caudally (Fig. 14B).

Male genitalia: Genital bulb brownish yellow, spherical. Epandrium gradually narrowing toward apex, with a rounded, U-shaped terminal emargination (Fig. 14C). Hypovalve slender, bearing long bristles along inner margin, nearly reaching apex of gonocoxite (Figs 5L, 14D). Gonostylus shorter than gonocoxite, with a well-developed trapezoidal basal process and a small sharp subtriangular median tooth. Parameres trifurcate: basal branch considerably short, hook-shaped; mesal and lateral branches curved inward, reaching or exceeding apex of gonocoxite. Ventral valves of aedeagus short; dorsal valves broadened and elongate, nearly reaching apex of gonocoxite (Figs 5L, 14D, 15A, B).

Female genitalia: Subgenital plate ovoid, terminating in a ligulate process, covered with long setae caudally (Figs 14E, 15C). Medigynium strongly sclerotized, with main plate rectangular distally, gradually constricted mesally and rounded basally. Posterior arms parallel and short, approximately half the length of main plate (Figs 6L, M, 14F).

DISCUSSION

Owing to highly intraspecific variations and interspecific similarities, species delimitation of *Dicerapanorpa* has been challenging. By integrating
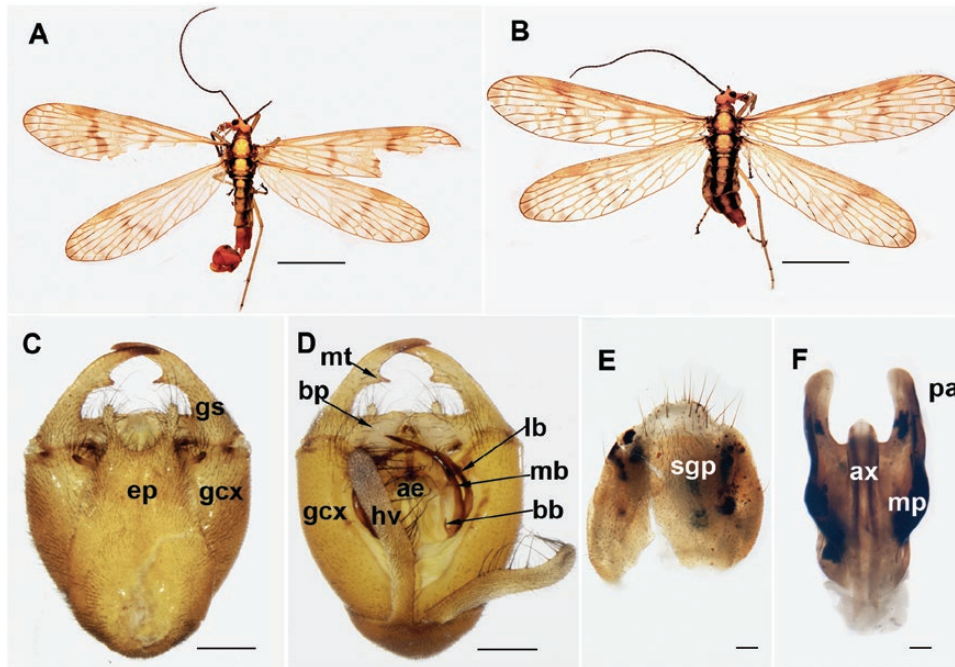
Figure 14. *Dicerapanorpa minshana*: A, male holotype, dorsal view; B, female paratype, dorsal view; C, D, male genital bulb, dorsal and ventral views, respectively; E, female subgenital plate, ventral view; F, female medigynium, ventral view. Abbreviations: ae, aedeagus; ax, axis; bb, basal branch; bp, basal process; ep, epandrium; gcx, gonocoxite; gs, gonostylus; hv, hypovalve; lb, lateral branch; mb, mesal branch; mp, main plate; mt, median tooth; pa, posterior arm; sgp, subgenital plate. Scale bars: 5.0 mm (A, B); 0.5 mm (C, D); 0.1 mm (E, F).
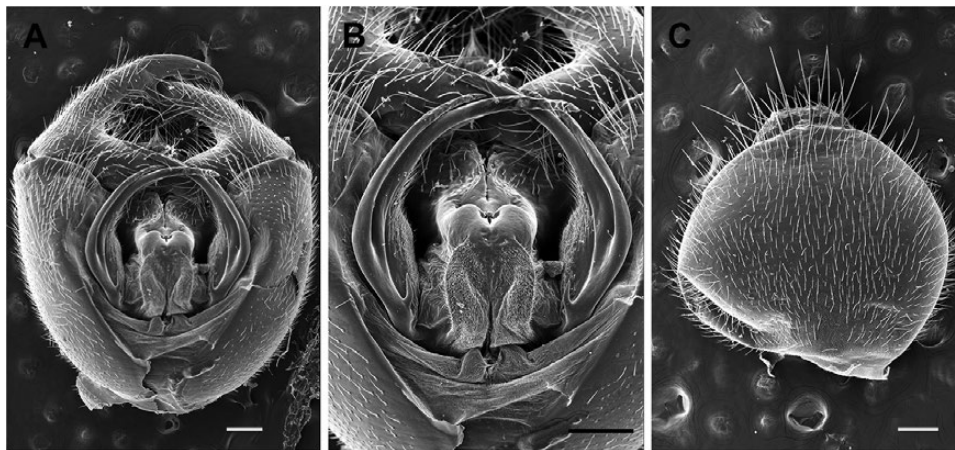
Figure 15. Scanning electron micrographs of male and female genitalia of *Dicerapanorpa minshana*: A, male genital bulb, with hypandrium removed, ventral view; B, magnification of A to show the male aedeagus and parameres, ventral view; C, female genital plate, ventral view. Scale bars: 0.2 mm.

molecular, morphological, geometric morphometric and phylogenetic analyses, this study confirmed the 13 species of *Dicerapanorpa* and revealed the existence of three formerly overlooked new species (*D. lativalva*, *D. hualongshana* and *D. minshana*), considerably deepening our understanding of species limits and boundaries in *Dicerapanorpa*.

Molecular approaches to species delimitation have developed rapidly in recent decades, and several methods are now available to infer species boundaries

(Dellicour & Flot, 2015). Our present study initially used the BIN system in BOLD to assign individuals to presumptive species, and subsequently applied three other delimitation methods (ABGD, GMYC bPTP). BIN unexpectedly grouped all samples of the five species in the *D. magna* group (clade IV in Fig. 2) together, which might result from the large geographical scale of sampling, as reported by Bergsten *et al.* (2012). The GMYC approach, especially the multiple-threshold model, greatly inflated the species count (30 OTUs), a result seen earlier in spiders (Satler *et al.*, 2013; Hedin, 2015). In contrast, bPTP produced a relatively conservative species count (18 OTUs) and was considered to outperform the GMYC model in both simulation and empirical studies (Zhang *et al.*, 2013; Hedin, 2015). The ABGD method was previously considered to perform poorly in delimiting species when sample sizes are low (fewer than five; Puillandre *et al.*, 2012b), but performed well in our study. These four methods are complementary, and effectively contribute to the final molecular OTUs.

The phylogenetic trees (Figs 8, 9) clearly indicate that the genus *Dicerapanorpa* is a monophyletic group, consistent with previous conclusions (Ma *et al.*, 2012; Hu *et al.*, 2015; Miao *et al.*, 2019). Clades I–III belong to the *D. diceras* group, and clade IV belongs to the *D. magna* group, showing the paraphyletic relationship of the *D. diceras* group with respect to the *D. magna* group. This might also suggest that the hyaline wings and the rostrum with two black longitudinal stripes in the *D. diceras* group are plesiomorphic characters, whereas the yellowish wings with distinct markings and the rostrum without stripes in the *D. magna* group are apomorphic characters.

Reciprocal monophyly is often viewed as the most important criterion for species delimitation (de Queiroz, 2007), but it is often not evident in recently diverged species (Knowles & Carstens, 2007; Cummings *et al.*, 2008). The phylogenetic trees (Figs 8, 9) in the present four-gene dataset reveal that some species are not monophyletic. For example, *D. shennongensis* is paraphyletic with *D. baiyunshana*, and *D. yijunae* is paraphyletic with *D. kimminsi*. The potential reason for this phenomenon might be hybridization followed by introgression, incomplete lineage sorting and recent evolutionary divergence, as explained in previous studies (Funk & Omland, 2003; Knowles & Carstens, 2007; Degnan & Rosenberg, 2009). New species start from initial polyphyly and achieve monophyly through paraphyly in the speciation process (Avise, 2000). The progress may be more rapid for mitochondrial haplotypes and can be distinctive in the case of budding speciation through peripheral isolation (Frey, 1993). Ancestral (e.g. *D. shennongensis*) and budding species (e.g. *D. baiyunshana*) will remain paraphyletic until the ancestral species has lost the characteristics

of the budding species (Podani, 2013; Kaya & Çiplak, 2016). Mitochondrial genes play a dominant role in the phylogenetic reconstruction, probably leading to discordance between the phylogenetic topology and species tree. Even so, the mitochondrial genetic data, as a source of complementation to other evidence for species delimitation, do provide valuable information for investigating evolutionary histories and patterns of species diversity (Avise, 2009; Monaghan *et al.*, 2009; Fujisawa & Barraclough, 2013).

Male genitalia are remarkably useful morphological traits for species discrimination (Song & Bucheli, 2010). Numerous taxa of insects have evolved species-specific male genitalia, and morphological divergence of male genitalia among closely related species is often dramatic (Eberhard, 1985). For example, body coloration and wing pattern are relatively conserved in *Dicerapanorpa*, whereas genital shape and complexity exhibit a greater divergence, as also seen in water striders (Eberhard, 2010; Rowe & Arnqvist, 2012). The paramere of male genitalia is the most phenotypically differentiated structure in *Dicerapanorpa*, with variation of its shape and length distinguishing closely related species, especially in the *D. magna* group (Fig. 5L–P). The rapid evolution and divergence of this trait have probably been driven by sexual selection through facilitating male domination and success in the process of copulation (Hosken & Stockley, 2004; Simmons, 2014). The male genital structures in scorpionflies, such as the gonostylus, hypovalve and epandrium, in addition to the anal horn and notal organ, have been shown to function in countering the female resistance and stabilizing the mating position (Ma *et al.*, 2010; Zhong & Hua, 2013b; Zhong *et al.*, 2015).

In contrast, female genital structures have been little studied by taxonomists, mainly because they are generally internal and require dissection (Simmons, 2014). The medigynium, an important component of female genitalia, was previously considered as possessing taxonomic value in scorpionflies (Byers, 1954; Cheng, 1957). Ma *et al.* (2012) concluded that the medigynium is a reliable character for species delimitation in the Panorpidae at generic or higher levels. The present study corroborates that most *Dicerapanorpa* species have a morphologically distinct medigynium, with considerable variation within some species, such as *D. magna* (Fig. 6O, P) and *D. shennongensis* (Fig. 6Q–S). The extensive morphological variations between and within populations in *Dicerapanorpa* are more complicated than the variation in male genitalia, a situation also noted in a scarab beetle (Polihronakis, 2009). The copulatory pore is situated at the posterior end of the axis of the medigynium in *Dicerapanorpa*, implying that the main plate and posterior arms are likely to be free from functional constraint. This might explain

the extensive variation in the shape and length of the female medigynium in *Dicerapanorpa*.

Evidence from multiple characters suggests that the *D. magna* group consists of five species, i.e. *D. baiyunshana*, *D. hualongshana*, *D. magna*, *D. minshana* and *D. shennongensis*. A previous geometric morphometric study of wings supports the significant differences between *D. hualongshana* and *D. magna* (Liu *et al.*, 2016). A phylogeographical study (Hu *et al.*, 2019a) also suggests the presence of three genetically distinct lineages and incipient speciation in the *D. magna* group (i.e. *D. hualongshana*, *D. magna* and *D. minshana*). Geographical barriers, including mountains and the Hanshui River between the Qinling and Bashan Mountains (Su *et al.*, 2015; Liu *et al.*, 2016), are apparently responsible for limiting gene flow and promoting divergence among species in the *D. magna* group. Pleistocene glaciations could also have promoted recent divergence associated with colonization of individual sky islands, as found in grasshoppers (Knowles, 2001). Owing to divergent ecological selection, reproductive isolation between allopatric populations might have evolved. However, *D. hualongshana*, *D. magna* and *D. minshana* have probably experienced recurrent range contractions and expansions during the Pleistocene, leading to secondary contact between allopatric populations (Hu *et al.*, 2019a). These species are probably able to hybridize in the contact zone, because they are unlikely to exhibit complete reproductive isolation.

Mountain regions, as naturally fragmented habitat islands, provide opportunities for new species to diversify and survive (Hewitt, 2000, 2004). Allopatric speciation is often fostered by geographical barriers within montane systems owing to natural selection or genetic drift (Vuilleumier & Monasterio, 1986; Moritz *et al.*, 2000), leading to the exceptionally high species diversity and richness in the mountains of southwestern China. Besides, the climate changes during the Pleistocene have probably contributed to population differentiation and speciation processes in *Dicerapanorpa* (Hu *et al.*, 2019a). The *Dicerapanorpa* species considered in this study are narrow endemics restricted to small or medium-sized regions on the mountaintops with a few exceptions in the *D. magna* group. Some species of *Dicerapanorpa* may have experienced convergent evolution, because they display nearly identical body and wing coloration, which might result from similar selective pressure in the mountain sky islands, as noted in cave-dwelling harvestmen (Derkarabetian *et al.*, 2010; Derkarabetian & Hedin, 2014). Nevertheless, the integrative approach has uncovered taxonomic boundaries in these morphologically conserved species, such as *D. diceras*, *D. lativalva* and *D. luojishana*, laying a foundation for future evolutionary and systematic studies of this group.

REFERENCES

Avise JC. 2000. *Phylogeography: the history and formation of species*. Cambridge: Harvard University Press.

Avise JC. 2009. Phylogeography: retrospect and prospect. *Journal of Biogeography* **36:** 3–15.

Bergsten J, Bilton DT, Fujisawa T, Elliott M, Monaghan MT, Balke M, Hendrich L, Geijer J, Herrmann J, Foster GN, Ribera I, Nilsson AN, Barraclough TG, Vogler AP. 2012. The effect of geographical scale of sampling on DNA barcoding. *Systematic Biology* **61:** 851–869.

Bickford D, Lohman DJ, Sodhi NS, Ng PK, Meier R, Winker K, Ingram KK, Das I. 2007. Cryptic species as a window on diversity and conservation. *Trends in Ecology & Evolution* **22:** 148–155.

Bortolus A. 2008. Error cascades in the biological sciences: the unwanted consequences of using bad taxonomy in ecology. *AMBIO: A Journal of the Human Environment* **37:** 114–118.

Byers GW. 1954. Notes on North American Mecoptera. *Annals of the Entomological Society of America* **47:** 484–510.

Carpenter FM. 1938. Mecoptera from China, with descriptions of new species. *Proceedings of the Entomological Society of Washington* **40:** 267–281.

Carstens BC, Pelletier TA, Reid NM, Satler JD. 2013. How to fail at species delimitation. *Molecular Ecology* **22:** 4369–4383.

Cheng FY. 1957. Revision of the Chinese Mecoptera. *Bulletin of the Museum of Comparative Zoology* **116:** 1–118.

Cummings MP, Neel MC, Shaw KL. 2008. A genealogical approach to quantifying lineage divergence. *Evolution* **62:** 2411–2422.

Darriba D, Taboada GL, Doallo R, Posada D. 2012. jModelTest 2: more models, new heuristics and parallel computing. *Nature Methods* **9:** 772.

Dayrat B. 2005. Towards integrative taxonomy. *Biological Journal of the Linnean Society* **85:** 407–415.

Degnan JH, Rosenberg NA. 2009. Gene tree discordance, phylogenetic inference and the multispecies coalescent. *Trends in Ecology & Evolution* **24:** 332–340.

Dejaco T, Gassner M, Arthofer W, Schlick-Steiner BC, Steiner FM. 2016. Taxonomist's nightmare … evolutionist's delight: an integrative approach resolves species limits in jumping bristletails despite widespread hybridization and parthenogenesis. *Systematic Biology* **65:** 947–974.

Dellicour S, **Flot JF. 2015.** Delimiting species-poor data sets using single molecular markers: a study of barcode gaps, Haplowebs and GMYC. *Systematic Biology* **64:** 900–908.

Derkarabetian S, **Hedin M. 2014.** Integrative taxonomy and species delimitation in harvestmen: a revision of the western North American genus *Sclerobunus* (Opiliones: Laniatores: Travunioidea). *PLoS ONE* **9:** e104982.

Derkarabetian S, **Steinmann DB**, **Hedin M. 2010.** Repeated and time-correlated morphological convergence in cave-dwelling harvestmen (Opiliones, Laniatores) from montane western North America. *PLoS ONE* **5:** e10388.

Drummond AJ, **Suchard MA**, **Xie D**, **Rambaut A. 2012.** Bayesian phylogenetics with BEAUti and the BEAST 1.7. *Molecular Biology and Evolution* **29:** 1969–1973.

Eberhard WG. 1985. *Sexual selection and animal genitalia*. Cambridge: Harvard University Press.

Eberhard WG. 2010. Evolution of genitalia: theories, evidence, and new directions. *Genetica* **138:** 5–18.

Folmer O, **Black M**, **Hoeh W**, **Lutz R**, **Vrijenhoek R. 1994.** DNA primers for amplification of mitochondrial cytochrome *c* oxidase subunit I from diverse metazoan invertebrates. *Molecular Marine Biology and Biotechnology* **3:** 294–299.

Frey JK. 1993. Modes of peripheral isolate formation and speciation. *Systematic Biology* **42:** 373–381.

Fujisawa T, **Barraclough TG. 2013.** Delimiting species using single-locus data and the Generalized Mixed Yule Coalescent approach: a revised method and evaluation on simulated data sets. *Systematic Biology* **62:** 707–724.

Funk DJ, **Omland KE. 2003.** Species-level paraphyly and polyphyly: frequency, causes, and consequences, with insights from animal mitochondrial DNA. *Annual Review of Ecology, Evolution, and Systematics* **34:** 397–423.

Glez-Peña D, **Gomez-Blanco D**, **Reboiro-Jato M**, **Fdez-Riverola F**, **Posada D. 2010.** ALTER: program-oriented conversion of DNA and protein alignments. *Nucleic Acids Research* **38:** W14–W18.

Goldstein PZ, **DeSalle R. 2011.** Integrating DNA barcode data and taxonomic practice: determination, discovery, and description. *Bioessays* **33:** 135–147.

Hall TA. 1999. BioEdit: a user-friendly biological sequence alignment editor and analysis program for Windows 95/98/NT. *Nucleic Acids Symposium Series* **41:** 95–98.

Hebert PDN, **Cywinska A**, **Ball SL**, **deWaard JR. 2003a.** Biological identifications through DNA barcodes. *Proceedings of the Royal Society B: Biological Sciences* **270:** 313–321.

Hebert PDN, **Ratnasingham S**, **deWaard JR. 2003b.** Barcoding animal life: cytochrome *c* oxidase subunit 1 divergences among closely related species. *Proceedings of the Royal Society B: Biological Sciences* **270**(Suppl 1)**:** S96–S99.

Hedin M. 2015. High-stakes species delimitation in eyeless cave spiders (*Cicurina*, Dictynidae, Araneae) from central Texas. *Molecular Ecology* **24:** 346–361.

Hewitt GM. 2000. The genetic legacy of the Quaternary ice ages. *Nature* **405:** 907–913.

Hewitt GM. 2004. Genetic consequences of climatic oscillations in the Quaternary. *Philosophical Transactions of the Royal Society B: Biological Sciences* **359:** 183–195.

Hosken DJ, **Stockley P. 2004.** Sexual selection and genital evolution. *Trends in Ecology & Evolution* **19:** 87–93.

Hou XY, **Hua BZ. 2008.** Structures of the female reproductive systems in Panorpidae (Mecoptera) with remarks on their taxonomic significance. *Acta Zootaxonomica Sinica* **33:** 427–434.

Hsu TH, **Ning Y**, **Gwo JC**, **Zeng ZN. 2013.** DNA barcoding reveals cryptic diversity in the peanut worm *Sipunculus nudus*. *Molecular Ecology Resources* **13:** 596–606.

Hu GL, **Hua BZ. 2019.** Two new species of the genus *Dicerapanorpa* (Mecoptera: Panorpidae) from Sichuan, China. *Entomotaxonomia* **41:** 73–79.

Hu GL, **Hua Y**, **Hebert PDN**, **Hua BZ. 2019a.** Evolutionary history of the scorpionfly *Dicerapanorpa magna* (Mecoptera, Panorpidae). *Zoologica Scripta* **48:** 93–105.

Hu GL, **Wang JS**, **Hua BZ. 2019b.** Five new species of *Dicerapanorpa* Zhong & Hua (Mecoptera, Panorpidae) from Yunnan, China. *Journal of Asia-Pacific Entomology* **22:** 159–166.

Hu GL, **Yan G**, **Xu H**, **Hua BZ. 2015.** Molecular phylogeny of Panorpidae (Insecta: Mecoptera) based on mitochondrial and nuclear genes. *Molecular Phylogenetics and Evolution* **85:** 22–31.

Isaac NJ, **Mallet J**, **Mace GM. 2004.** Taxonomic inflation: its influence on macroecology and conservation. *Trends in Ecology & Evolution* **19:** 464–469.

Katoh K, **Asimenos G**, **Toh H. 2009.** Multiple alignment of DNA sequences with MAFFT. *Methods in Molecular Biology* **537:** 39–64.

Kaya S, **Çiplak B. 2016.** Budding speciation via peripheral isolation: the *Psorodonotus venosus* (Orthoptera, Tettigoniidae) species group example. *Zoologica Scripta* **45:** 521–537.

Klingenberg CP. 2011. MorphoJ: an integrated software package for geometric morphometrics. *Molecular Ecology Resources* **11:** 353–357.

Knowles LL. 2001. Did the Pleistocene glaciations promote divergence? Tests of explicit refugial models in montane grasshoppers. *Molecular Ecology* **10:** 691–701.

Knowles LL, **Carstens BC. 2007.** Delimiting species without monophyletic gene trees. *Systematic Biology* **56:** 887–895.

Lanfear R, **Calcott B**, **Ho SYW**, **Guindon S. 2012.** PartitionFinder: combined selection of partitioning schemes and substitution models for phylogenetic analyses. *Molecular Biology and Evolution* **29:** 1695–1701.

Liu M, **Ma N**, **Hua BZ. 2016.** Intraspecific morphological variation of the scorpionfly *Dicerapanorpa magna* (Chou) (Mecoptera: Panorpidae) based on geometric morphometric analysis of wings. *Contributions to Zoology* **85:** 1–11.

Ma N, **Cai LJ**, **Hua BZ. 2009.** Comparative morphology of the eggs in some Panorpidae (Mecoptera) and their systematic implication. *Systematics and Biodiversity* **7:** 403–417.

Ma N, **Chen HM**, **Hua BZ. 2014.** Larval morphology of the scorpionfly *Dicerapanorpa magna* (Chou) (Mecoptera: Panorpidae) and its adaptive significance. *Zoologischer Anzeiger* **253:** 216–224.

Ma N, **Liu SY**, **Hua BZ. 2011.** Morphological diversity of male salivary glands in Panorpidae (Mecoptera). *European Journal of Entomology* **108:** 493–499.

Ma N, **Zhong W**, **Gao QH**, **Hua BZ. 2012.** Female genital plate diversity and phylogenetic analyses of East Asian Panorpidae (Mecoptera). *Systematics and Biodiversity* **10:** 159–178.

Ma N, **Zhong W**, **Hua BZ. 2010.** Genitalic morphology and copulatory mechanism of the scorpionfly *Panorpa jilinensis* (Mecoptera: Panorpidae). *Micron* **41:** 931–938.

Mendoza AM, **Torres MF**, **Paz A**, **Trujillo-Arias N**, **Lopez-Alvarez D**, **Sierra S**, **Forero F**, **Gonzalez MA. 2016.** Cryptic diversity revealed by DNA barcoding in Colombian illegally traded bird species. *Molecular Ecology Resources* **16:** 862–873.

Miao Y, **Wang JS**, **Hua BZ. 2019.** Molecular phylogeny of the scorpionflies Panorpidae (Insecta: Mecoptera) and chromosomal evolution. *Cladistics* **35**(4). doi: 10.1111/cla.12357.

Miller MA, **Pfeiffer W**, **Schwartz T. 2010.** Creating the CIPRES Science Gateway for inference of large phylogenetic trees. In: *Proceedings of the Gateway Computing Environments workshop (GCE)*. New Orleans: Institute of Electrical and Electronics Engineers, 1–8.

Monaghan MT, **Wild R**, **Elliot M**, **Fujisawa T**, **Balke M**, **Inward DJ**, **Lees DC**, **Ranaivosolo R**, **Eggleton P**, **Barraclough TG**, **Vogler AP. 2009.** Accelerated species inventory on Madagascar using coalescent-based models of species delineation. *Systematic Biology* **58:** 298–311.

Moritz C, **Patton J**, **Schneider C**, **Smith T. 2000.** Diversification of rainforest faunas: an integrated molecular approach. *Annual Review of Ecology and Systematics* **31:** 533–563.

Padial JM, **Miralles A**, **De la Riva I**, **Vences M. 2010.** The integrative future of taxonomy. *Frontiers in Zoology* **7:** 16.

Podani J. 2013. Tree thinking, time and topology: comments on the interpretation of tree diagrams in evolutionary/ phylogenetic systematics. *Cladistics* **29:** 315–327.

Polihronakis M. 2009. Hierarchical comparative analysis of genetic and genitalic geographical structure: testing patterns of male and female genital evolution in the scarab beetle *Phyllophaga hirticula* (Coleoptera: Scarabaeidae). *Biological Journal of the Linnean Society* **96:** 135–149.

Pons J, **Barraclough T**, **Gomez-Zurita J**, **Cardoso A**, **Duran D**, **Hazell S**, **Kamoun S**, **Sumlin W**, **Vogler A. 2006.** Sequence-based species delimitation for the DNA taxonomy of undescribed insects. *Systematic Biology* **55:** 595–609.

Puillandre N, **Lambert A**, **Brouillet S**, **Achaz G. 2012a.** ABGD, Automatic Barcode Gap Discovery for primary species delimitation. *Molecular Ecology* **21:** 1864–1877.

Puillandre N, **Modica MV**, **Zhang Y**, **Sirovich L**, **Boisselier MC**, **Cruaud C**, **Holford M**, **Samadi S. 2012b.** Large-scale species delimitation method for hyperdiverse groups. *Molecular Ecology* **21:** 2671–2691.

de Queiroz K. 2005. Ernst Mayr and the modern concept of species. *Proceedings of the National Academy of Sciences of the United States of America* **102**(Suppl 1)**:** 6600–6607.

de Queiroz K. 2007. Species concepts and species delimitation. *Systematic Biology* **56:** 879–886.

Ratnasingham S, **Hebert PDN. 2007.** BOLD: the barcode of life data system (http://www.barcodinglife.org). *Molecular Ecology Notes* **7:** 355–364.

Ratnasingham S, **Hebert PDN. 2013.** A DNA-based registry for all animal species: the barcode index number (BIN) system. *PLoS ONE* **8:** e66213.

Rohlf F. 2010. *TpsUtil v1.46*. Stony Brook: Department of Ecology and Evolution, State University of New York.

Rohlf F. 2015. *TpsDig2*. Stony Brook: Department of Ecology and Evolution, State University of New York.

Ronquist F, **Huelsenbeck JP. 2003.** MrBayes 3: Bayesian phylogenetic inference under mixed models. *Bioinformatics* **19:** 1572–1574.

Rowe L, **Arnqvist G. 2012.** Sexual selection and the evolution of genital shape and complexity in water striders. *Evolution* **66:** 40–54.

Satler JD, **Carstens BC**, **Hedin M. 2013.** Multilocus species delimitation in a complex of morphologically conserved trapdoor spiders (Mygalomorphae, Antrodiaetidae, *Aliatypus*). *Systematic Biology* **62:** 805–823.

Schlick-Steiner BC, **Steiner FM**, **Seifert B**, **Stauffer C**, **Christian E**, **Crozier RH. 2010.** Integrative taxonomy: a multisource approach to exploring biodiversity. *Annual Review of Entomology* **55:** 421–438.

Schutze MK, **Aketarawong N**, **Amornsak W**, **Armstrong KF**, **Augustinos AA**, **Barr N**, **Bo W**, **Bourtzis K**, **Boykin LM**, **Cáceres C**, **Cameron SL**, **Chapman TA**, **Chinvinijkul S**, **Chomič A**, **De Meyer M**, **Drosopoulou E**, **Englezou A**, **Ekesi S**, **Gariou-Papalexiou A**, **Geib SM**, **Hailstones D**, **Hasanuzzaman M**, **Haymer D**, **Hee AKW**, **Hendrichs J**, **Jessup A**, **Ji Q**, **Khamis FM**, **Krosch MN**, **Leblanc LUC**, **Mahmood K**, **Malacrida AR**, **Mavragani-Tsipidou P**, **Mwatawala M**, **Nishida R**, **Ono H**, **Reyes J**, **Rubinoff D**, **San Jose M**, **Shelly TE**, **Srikachar S**, **Tan KH**, **Thanaphum S**, **Haq I**, **Vijaysegaran S**, **Wee SL**, **Yesmin F**, **Zacharopoulou A**, **Clarke AR. 2015.** Synonymization of key pest species within the *Bactrocera dorsalis* species complex (Diptera: Tephritidae): taxonomic changes based on a review of 20 years of integrative morphological, molecular, cytogenetic, behavioural and chemoecological data. *Systematic Entomology* **40:** 456–471.

Schutze MK, **Virgilio M**, **Norrbom A**, **Clarke AR. 2017.** Tephritid integrative taxonomy: where we are now, with a focus on the resolution of three tropical fruit fly species complexes. *Annual Review of Entomology* **62:** 147–164.

Sheets HD. 2009. *MakeFan7*. Buffalo: Department of Physics, Canisius College.

Sheets HD. 2012. *IMP software series*. Buffalo: Department of Physics, Canisius College.

Silvestro D, **Michalak I. 2012.** raxmlGUI: a graphical front-end for RAxML. *Organisms Diversity & Evolution* **12:** 335–337.

Simmons LW. 2014. Sexual selection and genital evolution. *Austral Entomology* **53:** 1–17.

Simon C, **Frati F**, **Beckenbach A**, **Crespi B**, **Liu H**, **Flook P. 1994.** Evolution, weighting, and phylogenetic utility of mitochondrial gene sequences and a compilation of

conserved polymerase chain reaction primers. *Annals of the Entomological Society of America* **87:** 651–701.

Smith MA, **Woodley NE**, **Janzen DH**, **Hallwachs W**, **Hebert PDN. 2006.** DNA barcodes reveal cryptic host-specificity within the presumed polyphagous members of a genus of parasitoid flies (Diptera: Tachinidae). *Proceedings of the National Academy of Sciences of the United States of America* **103:** 3657–3662.

Song H, **Bucheli SR. 2010.** Comparison of phylogenetic signal between male genitalia and non-genital characters in insect systematics. *Cladistics* **26:** 23–35.

Song N, **Liang AP. 2013.** A preliminary molecular phylogeny of planthoppers (Hemiptera: Fulgoroidea) based on nuclear and mitochondrial DNA sequences. *PLoS ONE* **8**: e58400.

Su LN, **Li XC**, **Meng HZ**, **Gao XY**, **Yin H**, **Li K. 2015.** Population genetic structure and historical demography of the ground beetle *Chlaenius costiger* in the Tsinling-Dabashan Mountains of central China. *Genetics and Molecular Research* **14:** 3579–3589.

Swindell SR, **Plasterer TN. 1997.** SEQMAN. Contig assembly. *Methods in Molecular Biology* **70:** 75–89.

Vuilleumier F, **Monasterio M. 1986.** *High altitude tropical biogeography*. Oxford: Oxford University Press.

Wang JS, **Hua BZ. 2017.** An annotated checklist of the Chinese Mecoptera with description of male *Panorpa guttata* Navás, 1908. *Entomotaxonomia* **39:** 24–42.

Whiting MF. 2002. Mecoptera is paraphyletic: multiple genes and phylogeny of Mecoptera and Siphonaptera. *Zoologica Scripta* **31:** 93–104.

Wiens JJ. 2007. Species delimitation: new approaches for discovering diversity. *Systematic Biology* **56:** 875–878.

Witt JD, **Threloff DL**, **Hebert PDN. 2006.** DNA barcoding reveals extraordinary cryptic diversity in an amphipod genus: implications for desert spring conservation. *Molecular Ecology* **15:** 3073–3082.

Zhang J, **Kapli P**, **Pavlidis P**, **Stamatakis A. 2013.** A general species delimitation method with applications to phylogenetic placements. *Bioinformatics* **29:** 2869–2876.

Zhong W, **Ding G**, **Hua BZ. 2015.** The role of male's anal horns in copulation of a scorpionfly. *Journal of Zoology* **295:** 170–177.

Zhong W, **Hua BZ. 2013a.** *Dicerapanorpa*, a new genus of East Asian Panorpidae (Insecta: Mecoptera: Panorpidae) with descriptions of two new species. *Journal of Natural History* **47:** 1019–1046.

Zhong W, **Hua BZ. 2013b.** Mating behaviour and copulatory mechanism in the scorpionfly *Neopanorpa longiprocessa* (Mecoptera: Panorpidae). *PLoS ONE* **8:** e74781.

SUPPORTING INFORMATION

Additional Supporting Information is available in the online version of this article at the publisher's web-site:

Table S1. Detailed information for all specimens used for molecular analyses. *Samples are from previous phylogeographical study (Hu *et al.*, 2019a).

Table S2. Sequences for the forward (F) and reverse (R) primers used in this study.